Title: In Vivo Imaging of the Central and Peripheral Effects of Sleep Deprivation and Suprachiasmatic Nuclei Lesion on PERIOD-2 Protein in Mice.

Authors: Curie T, Maret S, Emmenegger Y, Franken P

Journal: Sleep

Year: 2015 Sep 1

Issue: 38

Volume: 9

Pages: 1381-94

DOI: 10.5665/sleep.4974

In vivo imaging of the central and peripheral effects of sleep deprivation and SCN lesion on PERIOD-2 protein in mice

Thomas Curie, Ph.D., Stephanie Maret, Ph.D., Yann Emmenegger, and Paul Franken, Ph.D.*

Center for Integrative Genomics, University of Lausanne, Switzerland

Short title
In vivo imaging of PER2 in sleep deprived mice

Disclosure Statement

This was not an industry supported study. The authors have indicated no financial conflicts of interest.

***Corresponding author**
Center for Integrative Genomics
University of Lausanne
1015 Lausanne, Switzerland
+41 21 692 3972
paul.franken@unil.ch

Abstract

Study objectives: That sleep deprivation increases the brain expression of various clock genes has been well documented. Based on these and other findings we hypothesized that clock genes not only underlie circadian rhythm generation but are also implicated in sleep homeostasis. However, long time lags have been reported between the changes in the clock gene mRNA levels and their encoded proteins. It is therefore crucial to establish whether also protein levels increase within the time frame known to activate a homeostatic sleep response. We report on the central and peripheral effects of sleep deprivation on PERIOD-2 (PER2) protein both in intact and SCN-lesioned mice.

Design: *In vivo* and *in situ* PER2 imaging during baseline, sleep deprivation, and recovery.

Settings: Mouse sleep-recording facility.

Participants: *Per2::Luciferase* knock-in mice.

Interventions: N/A

Measurements and Results: Six-hour sleep deprivation increased PER2 not only in the brain but also in liver and kidney. Remarkably, the effects in the liver outlasted those observed in brain. Within the brain the increase in PER2 concerned the cerebral cortex mainly, while leaving SCN levels unaffected. Against expectation, sleep deprivation did not increase PER2 in the brain of arrhythmic SCN-lesioned mice due to higher PER2 levels in baseline. In contrast, liver PER2 levels did increase in these mice similar to the sham- and partially-lesioned controls.

Conclusions: Our results stress the importance of considering both sleep-wake dependent and circadian processes when quantifying clock-gene levels. Because sleep deprivation alters PER2 in the brain as well as in the periphery, it is tempting to speculate that clock genes constitute a common pathway mediating the shared and well-known adverse effects of both chronic sleep loss and disrupted circadian rhythmicity on metabolic health.

Keywords: PER2 protein, *in vivo* imaging, bioluminescence, homeostasis, sleep deprivation, clock genes, cerebral cortex, hippocampus, cerebellum, Purkinje cells, SCN-lesion, circadian.

Introduction

The timing and quality of both sleep and wakefulness depend on the interaction of two processes. A sleep-wake driven process monitors and controls homeostatic sleep need, while a circadian process generates a sleep-wake independent wake-promoting signal. The circadian wake-promoting signal is thought to oppose homeostatic sleep need thereby determining the time-of-day sleep occurs.[1] Studies aimed at dissecting the respective contributions of sleep-wake dependent and circadian factors to sleep-wake regulation are hampered by the fact that many aspects of sleep are directly or indirectly affected by both processes. Accumulating evidence shows that even the so-called clock genes, long thought to encode circadian time information exclusively and therefore widely used as circadian state variables, are also implicated in the homeostatic process; i.e., conferring information concerning time-spent-awake (and asleep).[2]

The notion that clock genes play a role in the homeostatic aspect of sleep regulation comes from three types of observations. First, altered sleep homeostasis was observed in animals, including humans, carrying clock gene mutations or polymorphisms.[3-12] In these studies the response to sleep deprivation in terms of increased sleep duration and/or EEG delta power during NREM sleep, a widely used state variable of the sleep homeostatic process,[13] differed from those observed in controls. A second type of observation concerns the effects of sleep deprivation on the specific DNA-binding of NPAS2 and BMAL1 to the E-box motives of specific target genes, among which the clock gene *Per2*.[14] This study demonstrates that extended wakefulness directly affects the core clock machinery. Lastly, and likely related to the previous observation, the expression of a number of core circadian transcripts changes as a function of time-spent-awake (or time-spent-asleep). Among those, *Per2* mRNA levels in the brain are reliably and predictably increased by sleep deprivation under a number of conditions.[8,15-18]

From circadian time course analyses it is known that 6- to 8h lags exist between the time at which mRNA and protein levels peak for many clock genes.[19] These long time lags have been attributed to the many post-transcriptional and -translational processes known to modify the stability and nuclear entry of clock genes among other mechanisms.[19-21] In the mouse robust homeostatic responses in a variety of sleep variables can, however, already be observed after sleep deprivations of 6h.[22,23] If clock genes are to play a functional role in sleep homeostasis, their protein product should increase within such time frame. To date,

studies quantifying clock gene protein levels after sleep deprivation are lacking and a main aim of the present study is therefore to determine the dynamics of the protein levels of the clock gene *Per2* during sleep deprivation and recovery sleep. In addition, we have previously shown that the wake-dependent increase in *Per2* expression is modulated by circadian factors.[18] Hence, a further goal is to determine the influence of lesioning the supra-chiasmatic nuclei (SCN), the central circadian pacemaker, on the sleep-deprivation induced increase of PER2. We expect to observe this increase also in behaviourally arrhythmic mice. As accumulating evidence suggests that sleep deprivation not only affects gene expression in the brain but also in the periphery,[16,24-26] a last aim was to establish whether PER2 levels in the liver and kidney are affected as well.

To achieve these goals we used *Per2::Luciferase* (*Per2*^{Luc}) knock-in mice,[27] to image PER2 protein variations in the whole living mouse. We found that PER2 protein increases after sleep deprivation not only in the brain but also in the liver and the kidney, albeit with tissue specific dynamics. Brain immunohistochemistry established that sleep deprivation targeted PER2 levels in layers IV and V of the cerebral cortex, while levels in SCN remained unperturbed. These results demonstrate for the first time that in the brain, sleep deprivation rapidly increases PER2 (within 3h) and thus that the protein follows the changes in mRNA more closely as compared to the circadian relationship between the two. Against expectation, the sleep-deprivation induced increase of PER2 in the brain was smaller in SCN-lesioned mice while in the liver PER2 was again higher than baseline similar to sham- and partially-lesioned control mice. Equally unexpected was the finding that in some SCN-lesioned mice we could still identify circadian rhythmicity in PER2 despite an absence of a circadian organization of locomotor activity. Illustrated for *Per2*, these results stress the importance of considering both sleep-wake dependent and circadian processes when quantifying clock gene levels *in vivo*.

Experimental procedures

Animals, housing conditions and sleep deprivation (SD): All animals were kept under a 12h light/ 12h-dark cycle (LD12:12; lights on at 09:00, 110lx) and were singly housed with food and water available *ad libitum*. We use Zeitgeber time (ZT) to indicate time-of-day with ZT0 (or ZT24) marking light onset and ZT12 dark onset. Cages were placed in a sound attenuated

and temperature controlled recording room (25°C). Both female and male mice were used. Animals were sleep-deprived (SD) by what is referred to as 'gentle handling' [28].

C57BL/6J (B6) mice heterozygous for the *Per2::Luciferase* knock-in construct (*Per2*^{Luc}; kindly provided by Dr. J.S. Takahashi, University of Texas, Southwestern Medical Center, TX, USA) were bred in our facility and all experiments were approved by the Ethical Committee of the State of Vaud Veterinary Office, Switzerland. PCR genotyping was done as described previously.[27]

In vivo *PER2 bioluminescence imaging:* Mice heterozygous for the *Per2*^{Luc} construct displayed lower levels of bioluminescence (data not shown) and all experiments were therefore performed in homozygous *Per2*^{Luc} mice only. The luciferase substrate, D-luciferin (Prolume Ltd, Pinetop, AZ, USA; 35mg/mL diluted in ACSF, pH 7.3), was delivered using osmotic mini pumps (model 1002, Alzet, Cupertino, CA, USA; release rate 0.25µL/h over 14 days according to manufacturer's specifications). For brain delivery of D-luciferin, a cannula (Brain infusion kit1, Alzet) was introduced stereotaxically into the right lateral ventricle (1mm lateral, 0.3mm posterior to the bregma and 2.2mm deep) under deep anaesthesia (ketamine/xylazine; ip, 75 and 10mg/kg, respectively), and connected to the mini pump. Filled mini pumps were incubated in sterile saline solution at 37°C overnight prior to implantation. To facilitate passage of photons emitted by the brain through the skull, a depression (diameter 2mm^2) was made in (but not through) the skull in a region of the left frontal cortex (approximate coordinates 2mm lateral to midline, 2mm anterior to bregma), in which a glass cylinder (length 4.0mm; diameter 2.0mm^2) was positioned and fixed with dental cement. For peripheral organs, bioluminescence was detected directly through the skin in an abdominal region (2.0cm^2) corresponding to the liver and in a dorsal region (1.5cm^2) corresponding to the left kidney from the same mice. Pelage in these regions was removed.

For each reading, mice were lightly anesthetized (isoflurane; 2.5% vaporized in O_2). Bioluminescence was imaged with an ultra-sensitive CCD camera (IVIS 3D; field of view, 10; bin factor 2; Xenogen, Alameda, CA, USA). Light emission was integrated over 60s in triplicate and these triplicates were averaged yielding one measure per mouse and time point. The entire procedure did not last longer than 4min, after which mice were immediately returned to their home cage.

Bioluminescence readings from brain and peripheral organs in *Per2*^{Luc} mice (males and females, 3 months of age, brain: n=6/sex; liver and kidney: n=6/sex; total n=24), started 4 days after introducing the mini pump. Results did not differ with sex (analysis not shown). For the time course analyses during baseline, readings were obtained for 8 different times-of-day (ZT0, -3, -6, -9, -12, -15, -18, and -21) within each mouse spread out over a 4-day period such that no more than 2 measures were taken per day spaced at least 12h apart. Forty-eight hours after the last baseline reading, the same individuals were used to assess the effect of SD. First, control values were acquired the day prior to SD by imaging mice at ZT0, -6, -8, and -12. On the SD day (performed from ZT0 to -6) images were taken at ZT6, -8, and -12. For the sham, SCNx rhythmic and arrhythmic mice, the same protocol to quantify bioluminescence was performed but under complete darkness (DD) conditions.

For subsequent analysis, a large region of interest was drawn over the area of light emission and photon flux (photons/sec/cm^2/sr) was measured using Living Image^{TM} (Xenogen) as an overlay on Igor image analysis software (Wavemetrics, Inc, Lake Oswego, OR, USA). All measures were expressed as a percentage of the individual mean bioluminescence averaged over the 8 baseline values. With the concentration of D-luciferin used here, we found mean photon flux for bioluminescence to be at least 10-times higher than background (data not shown), which is consistent with the results described previously using the same concentration.[29] For 3D-reconstruction of bioluminescence source, see supplementary methods.

Day-to-day stability of bioluminescent signals was assessed in brain, liver, and kidney by imaging *Per2*^{Luc} mice (males, 3 months of age, n=7) daily for 21 days at ZT3 following osmotic mini-pump implantation. Signals were found to be stable between days 4 and 10 after mini pump implantation. This time-window was used for subsequent studies.

Immunohistofluorescence: Homozygous *Per2*^{Luc} mice were sacrificed at ZT0, -6, -12, and -18 and after SD (ZT0-6) at ZT6 *(*male, 3 months of age, n=3/time point; total n=15). All mice were subjected to intracardiac perfusion with PBS-heparin (2 units/ml) and with 4% paraformaldehyde in PBS, pH7.4. Brains were carefully removed and post-fixed for 3h at 4°C. Brains were cryoprotected in 10% and 20% of sucrose for 1h each and in 30% of sucrose in PBS for 48h at 4°C and then embedded in Tissue-Tek O.C.T. compound (VWR International, Switzerland) for cryostat sectioning.

Sagittal brain sections (30 µm) were washed in PBS (0.1% Triton X-100) and blocked (5% goat serum, Sigma Aldrich) and then incubated overnight at 4°C in a humidified chamber with primary antibodies directed against mPER2 (1:250; rabbit polyclonal IgG, Alpha Diagnostic international, ADi, San Antonio, TX, USA, and rabbit polyclonal IgG, 1:250, Santa Cruz, SC-25363, Heidelberg, Germany). The two antibodies yielded similar immunolabeling. Primary antibody against Vasopressin (AVP; 1:1000, guinea pig polyclonal anti-(Arg^8)-Vasopressin; Peninsula Laboratories, LLC, San Carlos, CA, USA) was used to identify the SCN. Sections were incubated at room temperature for 2h with Alexa-488 and Cy3-conjugated secondary antibodies [1:1000, Alexa Fluor® 488 goat anti-rabbit IgG (Invitrogen) and 1:1000, Cy3® polyclonal goat anti-guinea pig IgG (Abcam)]. Finally, sections were incubated with the nucleic acid counterstain DAPI (1:1000, room temperature, 5min, Vector laboratories), washed, and cover-slipped using Mowiol medium (Polyvinyl alcohol 4-88, Aldrich). Controls were performed by omitting primary antibodies, which in all cases resulted in an absence of immunofluorescence signal (not shown).

Fluorescence from whole brain sagittal views was acquired using a stereomicroscope MZ16FA (Leica). All other acquisitions were done with a confocal microscope (Zeiss 510 LSM). For triple-labeling with two antibodies plus DAPI, the 405-, 488-, and 543nm lines were used in alternating acquisition mode. For semi-quantitative analyses of the fluorescence for PER2, five sagittal slides per animal (total, n=15 slides) were selected containing the SCN and the hippocampus. For each slide, quantification of fluorescence for mPER2 was performed in five regions of interest (ROI): cerebral cortex, cerebellum, SCN, and the hippocampal *cornu ammonis* (CA) and dentate gyrus (DG) regions. In each sagittal slide, a ROI (1024 x 1024 pixels) was defined and a projection of 10 stacks was performed using a confocal microscope with the same optical stack distance for all acquisitions. Power of the lasers, opening of the pinhole, and detector gain were kept identical for all acquisitions. Z-stacks projections were exported in ImageJ 1.33u software to measure the MIP (Maximum Intensity Projection). Finally, data were z-transformed prior to statistical analyses.

SCN lesions, locomotor activity, and histology: Bilateral lesion of the two SCNs was performed stereotaxically (Kopf Instruments, 963LS, Miami Lakes, Florida, USA) under ketamine/xylazine aneasthesia (intraperitoneal injection, 75- and 10mg/kg, at a volume of 8ml/kg). Two electrodes (0.3mm in diameter) were introduced bilaterally at the following

coordinates (antero-posterior using bregma as reference: +0.5mm, lateral: 0.2mm, depth: 5.9mm). Electrolytic lesions (1mA, 5sec) were made using a DC lesion device (3500, Ugo Basile, Comerio, Italy). Sham mice differed from SCN lesioned mice only in that no electrical current was applied.

Locomotor activity of *Per2*^{Luc} mice (age 3-4 months) was recorded under a 12:12h light-dark conditions (LD12:12, lights on at 09:00, 110lux) at least for 10 days before lesion. After lesion, mice stayed 3-4 days under LD12:12, followed by constant dark (DD) conditions for 3 weeks to verify presence or absence of circadian organization of overt behavior. Activity was quantified using passive infra-red (PIR) sensors (Visonic SPY 4/RTE-A, Riverside, CA, USA). ClockLab software (Actimetrics, Wilmette, IL, USA) was used for data acquisition and analyses. The anatomical site of lesion was verified with Nissl staining on coronal brain sections (see Supplementary Figure S5).

At the end of the experiments, mice were anaesthetized with ketamine/xylazine (intraperitoneal injection, 75- and 10mg/kg, at a volume of 8mL/kg) and perfused intracardiacally with PBS-heparin (2units/mL) and with 4% paraformaldehyde in PBS, pH7.4. Brains were carefully removed and incubated in 10% and 20% of sucrose for 1h each, and in 30% of sucrose in PBS for 48h at 4°C, and then embedded in O.C.T. compound (VWR International, Switzerland) at -20°C until cryostat sectioning.

Coronal brain sections (20 µm) were washed in PBS and then post-fixed in PFA 4% at 4°C for 10 minutes. Brain sections were then incubated for 10-15 minutes in Cresyl violet (Sigma-Aldrich®) and washed in distilled water. Then brain slides were successively immerged in ethanol 95%, ethanol 100%, and three xylene baths before to be cover-slipped in Eukitt medium (Fluka). Chemical staining from whole brain coronal views was finally acquired using a Leica stereomicroscope (MZ16FA) and a Zeiss microscope (LSM510; Oberkochen, Germany) with Axiovision software.

Statistics: Statistical analyses were performed using SAS (SAS Institute Inc, Cary, NC, USA). Significant effects of the factors sleep deprivation and time-of-day and their interactions were assessed using ANOVA analyses (SAS, procedure GLM) and decomposed using post-hoc (paired) t-tests or Tukey's HSD tests in case more than 2 groups were compared. Statistical significance was set to $P<0.05$ and results are reported as mean $\pm$ SEM. Circadian rhythmicity in locomotor activity was evaluated using chi-square periodogram analysis ($P<0.05$; Clock

lab, Actimetrics, Wilmette, IL, USA). To estimate PER2-bioluminescence rhythmicity in intact, sham-lesioned, and SCN lesioned mice, sine waves were individually fit (SAS, procedure NLIN) to the 8 data obtained in each organ (liver, kidney, brain) with amplitude and phase as free parameters. As an estimate of period, the period length of the individual's rhythm in locomotor activity was used, which for the intact mice under LD12:12 was set to 24.0h. For arrhythmic SCN lesioned animals the average period of the sham-lesioned mice was used. When the estimated 95% confidence interval for the sine-wave amplitude did not overlap 0, bioluminescence was deemed rhythmic. SigmaPlot 11 (Systat Software Inc., Chicago, Il, USA) was used for graphs.

Results

The PER2::LUC fusion protein did not appear to interfere with PER2's clock function judged by the intact circadian locomotor activity patterns observed in *Per2*^{Luc} mice ([27] and Figure S1). Moreover, the baseline amount and distribution of sleep, the response to a 6h sleep deprivation (SD), and the sleep-wake driven changes in EEG delta power all indicate that also sleep regulation was not affected (Figure S1).

Subcutaneous delivery of D-luciferin, the substrate of luciferase, in *Per2*^{Luc} mice resulted in a strong bioluminescence signal throughout the body confirming the ubiquitous expression of PER2::LUC and, by inference, PER2 protein in wild-type mice.[27] Strongest bioluminescence signals were observed in two dorsal and one ventral region. Three-dimensional reconstruction identified the kidney and liver as their respective source (Figure S2). Bioluminescence levels were lowest in the head because the skull bone limits photon passage. Therefore, in a separate group of mice, the skull was thinned and equipped with a glass cylinder to assess brain PER2-bioluminescense (Figure 1A). Stable bioluminescence levels in brain, liver, and kidney were reached by day 4 after the start of luciferin delivery and maintained until day 10 (Figure S2). All subsequent experiments were performed within this 7-day window following the protocol illustrated in Figure S3.

In vivo assessment of the effects of time-of-day and sleep deprivation on PER2 protein under entrained conditions

The *in vivo*, nychthemeral changes in PER2 protein levels were quantified in brain, liver, and kidney. Robust, 3-fold changes in PER2 were observed in all three tissues with a nadir reached in the middle of the light-period (ZT6), while maximal levels were reached 3h after dark onset (ZT15) in the kidney and 3h before light onset (ZT21) in the liver and brain (Figure 1B). These changes in PER2 bioluminescence were similar in phase and amplitude to the changes obtained by western-blot analyses in a small subset of mice (Figure S4). This indicates that turnover of the PER2::LUC fusion protein and of the native PER2 protein are regulated in similar fashion and can be reliably monitored by bioluminescence *in vivo*.

We have previously shown that enforced wakefulness (i.e., sleep deprivation) increases *Per2* mRNA levels in the brain[8,10,15-18] suggesting that the nychthemeral sleep-wake distribution contributes to the nychthemeral (and circadian) changes in PER2 protein levels described here and previously by others.[30] The resemblance among the baseline time courses of locomotor activity, wakefulness, and PER2 levels, particularly in the brain, already support this (Figures 1 and S2). To further investigate this relationship, mice were sleep deprived (SD) for 6h (ZT0-6). Sleep deprivation was followed by an increase in PER2 levels not only in the brain, but also in liver and kidney, although the dynamics of this change during recovery sleep greatly varied among the three tissues (Figure 1C). In the brain, SD greatly attenuated the pronounced decrease in PER2 observed during corresponding baseline hours and 1.8-fold higher PER2 levels were observed immediately after SD, consistent with the about 2-fold increase in *Per2* mRNA levels observed after SDs performed at this time of day.[8,10,15-18] Brain PER2 levels were still increased after 2h of recovery sleep (ZT8) before reverting to baseline over the 4 subsequent recovery hours (Figure 1). Sleep deprivations as short as 3h are sufficient to increase *Per2* mRNA.[15] In a separate group of mice, we confirmed that 3h also suffices to fully counter the profound decrease in PER2 occurring between ZT0-3 (blue data point in the Figure 1B), suggesting that the sleep-wake driven changes in PER2 translation closely follow the changes in mRNA contrasting the long time-lag between the two reported for their circadian dynamics.[21,31]

Surprisingly and in stark contrast to the PER2 dynamics in the brain, liver levels remained elevated above baseline for the entire 6h over which recovery was measured while in kidney, a significant increase was observed at ZT8 only; i.e., after 2h of recovery sleep. Western-blot analysis of liver confirmed these bioluminescence results including the prolonged increase in PER2 after SD (Figure S4).

Brain topography of the PER2 increase after sleep deprivation

We then determined which brain areas contributed to the SD-induced changes in brain PER2 bioluminescence using immunohistofluorescence. Sleep deprivation increased PER2 fluorescence in the cerebral cortex, especially in the cingulate and motor cortices, the olfactory bulb, and cerebellum (Figure 2A). Close inspection of the brain areas directly under the site at which bioluminescence was sampled *in vivo* (see Methods); i.e., the cerebral cortex and the hippocampal fields CA1-3 and dentate gyrus, revealed that PER2 positive cells in cortical layers IV and V showed stronger fluorescence after SD as compared to baseline (Figures 2B and 3B; quantified in Figure 3G). Both the cell nuclei (co-localization with DAPI) and cytoplasm of these cells stained positive for PER2, with no apparent labeling of axonal projections (Figures 2B and 3B). PER2 positive cells were also found in the pyramidal cell layer throughout the CA fields of the hippocampus (Figures 2E and 3E). The cytoplasm, nucleus, and axonal projections of these cells stained all positive for PER2 (Figure 3E). PER2 staining was also observed in the granular cell layer and hile of the dentate gyrus (Figures 2F and 3F). Sleep deprivation did, however, not significantly modify PER2 staining in these hippocampal areas (Figures 2E and 2F; quantified in Figure 3G). It thus seems that the specific increase in PER2 expression in the cerebral cortex underlies the increase in bioluminescence observed in the brain *in vivo*.

Sleep deprivation increased PER2 also in the cerebellum (Figures 2A and 2D) although this increase failed to reach significance levels when quantified in the defined region of interest (Figure 3G). Visually identified Purkinje cells displayed a particularly strong PER2 fluorescence signal in the cytoplasm and axonal projections while in the nucleus PER2 was conspicuously absent (Figure 3D), contrasting the observations made in cerebral cortex and hippocampus. This absence of nuclear PER2 was noticed also at the other 3 times-of-day (data not shown).

Because SD can alter the phase of circadian activity rhythms[32] and affects multi-unit activity in the SCN[33], SD-dependent changes in PER2 in the SCN were anticipated. At the sagittal plane depicted (0.10-0.15mm lateral to midline), the SCN can be clearly discerned by the denser DAPI staining and the presence of vasopressin (AVP), which is specific of the dorso-medial region of the SCN (in red; Figures 2A and 2C). Most SCN cells positive for PER2 also stained for AVP but PER2 was clearly expressed in both the nucleus and cytoplasm,

whereas AVP is mainly cytoplasmic (Figure 3C). At the end of the SD (ZT6), only few PER2-positive cells were observed in the SCN and PER2 fluorescence after SD did not differ from that observed during baseline (Figures 2C and 3G). The lack of an effect of SD on PER2 levels in the SCN, along with decreased neuronal activity in the SCN,[33] could point to a dissociation of the molecular circadian clock from its neuronal output.

We then followed the changes in brain topography of PER2 expression over the day. In general, expression was highest and most wide-spread at ZT18 and lowest at ZT6 (Figure 3A). Nevertheless, quantification of these expression profiles showed that changes in fluorescence differed across the five areas for which it was quantified. No statistical variation in PER2 levels were observed in the dentate gyrus contrasting the large, 4.7-fold peak-to-trough changes observed in the SCN with maximal levels reached at ZT12 and minimal values at ZT0 (Figures 3C and 3G). Timing of peak and trough values varied among the other structures quantified (cerebellum: ZT18 and -12; CA: ZT0 and -12; cerebral cortex: ZT18 and -6, respectively). Of these profiles, the time-course of PER2 fluorescence in the cerebral cortex matched the changes of brain bioluminescence in *Per2*^{Luc} mice best (Figure 1B), again underscoring that the bioluminescence signal we quantified originated there.

Because the time-spent-awake and -asleep varies as a function of time-of-day and because enforced waking increases PER2 in the brain, the baseline sleep-wake distribution is likely to have contributed to these nycthemeral changes in PER2 expression. We therefore compared the SD-induced regional changes in PER2 expression to those observed after an extended period of spontaneous wakefulness like is the case at ZT18. High PER2 levels were observed both after SD and at ZT18 in the cerebral cortex, the cerebellum, and olfactory bulb (Figures 2A and 3A) and the levels quantified in the cortical and cerebellar regions (Figure 3G) indicated that spontaneous and enforced waking similarly contributed to the high PER2 levels in these areas. Despite these similarities between enforced and spontaneous periods of wakefulness with respect to PER2 levels, the important and widespread PER2 expression observed at ZT18, especially noticeable in the mid-brain and pontine areas, was conspicuously absent at ZT6 after the SD. Finally, PER2 in the SCN did not seem to be affected by sleep-wake states as highest levels were reached after the main rest phase and decreased over the main active period (Figures 3C and 3G), consistent with the fact that SD does not affect PER2 levels in this structure.

***In vivo* PER2 assessment in SCN-lesioned *Per2*^{Luc} mice under constant-dark conditions**

Next we studied the relationship between wakefulness and PER2 levels under constant dark (DD) conditions when circadian rhythms free-run. We also assessed the effects of lesioning the SCN (SCNx) (or the lack of circadian rhythms in locomotor activity), on PER2. Under DD conditions all *Per2*^{Luc} sham-operated mice displayed robust, circadian locomotor activity patterns resembling those observed in intact mice (Figures 4B and S5). Of the SCNx mice 53% still displayed significant rhythmicity albeit less robust statistically, likely due to incomplete lesioning of the SCN (for χ^2-analysis and histology see Figure S5). Average free-running periods did not differ between sham and rhythmic SCNx (rhySCNx) mice (24.2 ± 0.1h and 24.0 ± 0.1h, respectively). Compared to the LD12:12 condition, under DD the active period (alpha) expanded in both sham and partial lesioned mice (12.0 ± 0.1h *vs.* 14.8 ± 0.3h and 14.9 ± 0.4h, respectively; 1-way ANOVA $p<0.0001$; LD < sham = rhySCNx; post-hoc Tukey, $p<0.05$) increasing the time between the first main activity bout defining activity onset and the second main activity bout preceding rest onset. As a result, the bi-modal distribution of locomotor activity, already noticeable under LD12:12 (Figure 1D), became more pronounced especially in rhythmic SCNx mice (Figure 4B). In the arrhythmic SCNx mice no circadian organization of locomotor activity was detected and histological analyses did not reveal any remaining SCN tissue (Figure S5).

Following the same protocol used for the LD12:12 experiments (Figure S3), *in vivo* changes in PER2 bioluminescence were quantified over the circadian day in brain, liver, and kidney under DD conditions. For sham and rhythmic SCNx mice, average circadian PER2 profiles were constructed using individual period and phase information from the locomotor activity rhythms with circadian time 12 (CT12) as activity onset. In sham mice clear circadian PER2 patterns were readily discerned which paralleled activity patterns in similar fashion as under LD12:12 (Figure 4A, see Figure 1B for comparison). This included the bimodality in activity observed under DD, as also PER2 bioluminescence profiles showed two peaks in the active period, especially clear in kidney. Timing of the peak in the active phase, and the trough in the rest phase, were also similar as under LD12:12 while peak-trough amplitudes were somewhat smaller under DD conditions (2.4-, 2.2-, 1.9-fold for brain, liver, and kidney, respectively *vs.* 3.0-fold under LD12:12). Also in rhythmic SCNx mice, we observed circadian changes in PER2 similar to sham mice in all three organs but again with a smaller fold-change [1.9-, 1.7-, and 1.7-fold in brain, liver, and kidney, respectively; 2-way

ANOVA on the peak-trough amplitudes with factors 'Group' (LD, sham, rhySCNx; P=0.0015) and 'Tissue' (brain, liver, kidney; p=0.0031); interaction p=0.83; post-hoc Tukey; Group: LD > rhySCNx; Tissue: Brain > Kidney; $p<0.05$]. Also the analyses of the amplitude of sine-wave functions fitted to the changes in PER2 confirmed that amplitude decreases from intact mice under LD12:12 to sham mice under DD, to rhythmic SCNx mice under DD (Table 1).

In arrhythmic SCNx (arrSCNx) mice, no apparent circadian rhythm in PER2 bioluminescence was present in any of the three tissues (Figure 4A). However, since no activity rhythms were present, time courses of individual mice could not be aligned in a meaningful manner and we resorted to constructing average temporal PER2 profiles using average activity onset and period length of the rhythms observed in the sham-operated mice recorded in parallel. To address this limitation, we analyzed rhythmicity in all individual mice of the four experimental groups (LD, sham, rhySCNx, and arrSCNx) using a simple sine-wave fitting procedure (see Methods and Table 1 for details). Due to the sparsity of data (only eight samples covering one cycle per tissue and mouse) and due to the strong bimodality in PER2 that precluded fitting a sine function in some individuals, significant rhythms were not always obtained although clear rhythms being present visually. Despite these shortcomings, this method confirmed that under LD12:12 all tissues of all mice displayed PER2 rhythms to which a sine wave with an amplitude significantly deviating from zero could be fitted (Table 1). In the arrhythmic SCNx group, none of the liver recordings met this criterion while in brain and kidney PER2 changes were still deemed rhythmic in 14 (1/7) and 40% (2/5) of the mice, respectively.

Effects of DD and SCNx on the sleep-deprivation induced increase in PER2

In a final experiment we repeated the sleep deprivation under constant dark conditions to rule out eventual effects of light and entrainment. Moreover, we assessed whether an intact SCN (or a circadian organization of sleep-wake behavior) is required for the effects of sleep loss on PER2 expression. Consistent with the SD experiment under LD12:12, the 6h SD was scheduled from CT0-6. Since the active period expanded by almost 3 (circadian) hours under DD compared to LD12:12 (see above), the start of the SD no longer coincided with the onset of the rest phase. Nevertheless, under both DD and LD12:12 conditions the SD took place during the time PER2 levels steeply declined and both resulted in very similar, tissue-specific recovery dynamics (Figure 5 *vs.* Figure 1B). In sham-operated mice PER2 levels reached at

the end of the SD were again largest in brain of the sham mice after which they reverted to baseline levels over the following 6h. In kidney, changes were largest at CT8, and in liver PER2 remained elevated for the entire 6h recovery period as under LD12:12.

In rhythmic SCNx mice, PER2's response was very similar albeit less pronounced (Figure 5). This reduced response to SD was not due to differences in the PER2 values reached during recovery as they did not differ for any of the three time points and tissues among the three groups [2-way ANOVA with factors 'group' (sham, rhySCNx, arrSCNx), time (CT6, -8, and -12) for SD condition: 'group' p=0.60, 0.29, and 0.08 for brain, liver, and kidney, respectively]. Instead, this reduced relative increase was due to the fact that in rhythmic SCNx mice the PER2 values during baseline did not drop to the low values reached in sham mice [ANOVA for baseline condition: 'group' p=0.02, 0.01, and 0.005, for brain, liver, and kidney, respectively; post-hoc Tukey, $p<0.05$; *CT0: brain and kidney*: sham = rhySCNx > arrSCNx; *liver*: sham > arrSCNx; *CT6: brain*: arrSCNx > rhySCNx = sham; *CT8: kidney*: arrSCNx > rhySCNx = sham; *liver:* arrSCNx = rhySCNx > sham; *CT12: kidney*: rhySCNx > sham]. In arrhythmic SCNx mice, this baseline decrease in PER2 did not occur and during recovery from SD only modest effects were observed (Figure 5). Nevertheless, significant increases were also observed in this group, especially in the liver where after 2- and 4h of recovery PER2 levels were still increased over basal levels.

Discussion

In circadian research, live imaging of reporter genes has been widely used (e.g.[34,35]) and contributed to the rapid progress in that field. In animals these techniques were applied first *in vitro* and *ex vivo* in cells and tissues (e.g.[27,36,37]), and more recently, *in vivo* in the whole living organism.[29,38-40] In these *in vivo* studies circadian changes in bioluminescence could be followed in specific tissues of interest such as SCN, olfactory bulb, liver, and kidney. Because the same animal can be repeatedly sampled, these imaging techniques have an important advantage over more conventional techniques to quantify protein in that only a fraction of animals are needed to construct a circadian time course, and between-subject differences can be taken into account, thereby improving data quality. With the protocol we established, highly stable levels of bioluminescence could be maintained for the seven days without

further intervention. Variability in relative bioluminescence among individuals was small with a coefficient of variation typically around 20% for any given time point.

In the sleep field, *in vivo* measurement of protein expression in the intact animal has not yet been widely applied. We here report on the central and peripheral effects of sleep deprivation on PER2 protein levels under standard light-dark conditions and under constant dark conditions both in intact and SCN-lesioned mice. We discovered that similarly to mRNA, PER2 protein in the brain quickly increases with sleep deprivation and that this increase concerns the cerebral cortex mainly. These results further add to the notion that clock genes not only play a role in circadian rhythm generation but also in the homeostatic regulation of sleep.[2] Moreover, we found that sleep deprivation not only targets the brain but also peripheral tissues. Finally, we investigated the consequences of a SCN lesion on circadian- and wake-dependent changes in PER2. In three mice, significant PER2 circadian rhythmicity could still be detected in brain and kidney while rhythms in locomotor activity were lacking. Against expectation, sleep deprivation in arrhythmic SCNx mice resulted only in a modest relative increase in PER2 expression, mostly in liver, due to the higher baseline PER2 levels in this experimental group.

Comparing the effects of sleep deprivation on *Per2* mRNA and protein levels

The wake-dependent increase in *Per2* expression has been documented in a number of studies under a variety of experimental conditions demonstrating that both circadian and activity-induced contributions have to be considered when analyzing *Per2*'s time course.[18] If *Per2* is to play a functional role in sleep homeostasis, also its protein product should increase within the time frame known to activate a homeostatic response in sleep. From circadian time course analyses in; e.g., the SCN, it is known, however, that a long, 6- to 8h lag exists between the time at which *Per2* mRNA and PER2 protein peak.[19] Comparing our previous mRNA work with our current protein results, we confirmed the existence of such long time lag also in the brain; whereas mRNA started to decrease at ZT18,[18] the marked decrease in PER2 started 6h later; i.e., at ZT0 (or CT0 under constant dark conditions). In our study, higher than baseline levels of PER2 were already observed after a 3h sleep deprivation similarly to *Per2* mRNA,[15] suggesting that PER2 protein closely follows mRNA changes when activated through non-circadian pathways. Similarly, light-induced increases in PER2 protein in the SCN occurs within 4h[41,42] and corticosterone-induced increases in PER2 in specific

brain areas have been reported to occur within 1h.[43] These findings underscore that *Per2* has immediate-early gene properties when activated through non-circadian signaling pathways, which modulate and are modulated by the ongoing circadian rhythm in PER2. We have previously quantified and successfully mathematically modeled this non-linear interaction between circadian and activity-induced factors that determine *Per2* mRNA levels.[18] Based on the limited available data, the recovery dynamics of mRNA and protein seem to be less tightly coupled; whereas after 2h of recovery sleep *Per2* mRNA levels did already revert to baseline, for PER2 protein baseline levels were attained 4h later.

Sleep loss increases PER2 in the cerebral cortex

Within the brain the cerebral cortex, especially its layers IV and V, was most responsive to sleep loss in terms of the changes in PER2 levels. Given PER2's immediate-early gene properties (see above), increased expression in these two cortical layers could reflect increased sensory input (layer IV) and motor output (layer V)[44] associated with the sleep deprivation protocol. In contrast to the prominent changes observed in the cortex, sleep deprivation did not affect PER2 levels in the SCN. At the mRNA level similar dissociations between *Per2* expression rhythms in cortex and SCN have been observed under conditions of food restriction, spontaneous splitting, and methamphetamine administration where, invariably, expression in the cortex follows behavior (locomotor activity), while in the SCN its rhythm remains unperturbed and entrained to the light-dark cycle.[45-48] Functionally this makes intuitive sense as the SCN is required for time keeping and should therefore be shielded from the influence of the behaviors it drives. In contrast, we previously argued that in forebrain areas circadian clock genes are necessary to adapt to and anticipate homeostatic challenges such as food restriction and sleep deprivation.[10,30,49,50] The predominant effects of sleep deprivation on PER2 in the cerebral cortex is consistent with the many cortical related functions and activities that are affected by acute sleep deprivations, including increases in EEG slow waves, cognitive performance, and energy metabolism.[51]

In the cerebral cortex, similar levels of PER2 protein were reached immediately after enforced and spontaneous periods of wakefulness underscoring that at least a part of the variation in PER2 are secondary to the distribution of sleep and wakefulness and not primarily circadian driven. It is important to note that while animals are awake during sleep

deprivation, they will immediately revert to sleep when not stimulated, especially toward the end of the sleep deprivation. In contrast, during spontaneous waking, 'stimulation' can be said to be endogenous. The important and widespread PER2 expression observed at ZT18, especially clear in the mid-brain and pontine areas was conspicuously absent after the SD at ZT6. These areas contain several structures known to play important roles in the promotion of wakefulness and in sustained attention.[52] Thus, sleep deprivations performed during the rest phase, while activating the cerebral cortex, leave the rest of the brain molecularly asleep based on the PER2 levels measured here. These areas could be involved in mediating circadian wake-promotion that we observed at this time of day.[18]

Apart from the SCN, the most important nychthemeral changes in PER2 were observed in the cerebral cortex and cerebellum whereas no rhythmic expression was found in the hippocampus confirming previous studies and suggesting different physiological roles for PER2 in these brain regions.[53-55] Also the subcellular localization of PER2 differs among the brain regions evaluated here. In cortex and the SCN, neuronal PER2 is mainly nuclear and expressed in the perikaryon. In stark contrast, in cerebellar Purkinje neurons, PER2 is mainly cytoplasmic and expressed in projections but lacking from the nucleus as has been shown in one other study.[56] The absence of PER2 in the nucleus was observed at all times of day and is particularly surprising because, as a core circadian transcriptional regulator, PER2's nuclear presence is essential,[21] and because the strong PER2 rhythms observed in Purkinje neurons are functionally important in circadian food anticipatory behavior.[55] Whether in Purkinje cells other CLOCK::BMAL1 and CLOCK::NPAS2 repressors, such as PER1, are expressed in the nucleus and thus could substitute for the absence of PER2, is unknown.

The effects of sleep loss on PER2 in SCNx mice

Sleep deprivation performed between ZT0 and -6 (or CT0 and -6), efficiently countered the marked decrease in PER2 occurring at this circadian phase resulting in higher than baseline levels both centrally and peripherally. However, in the absence of this baseline decrease, such as in the arrhythmic SCNx mice, sleep deprivation did not appreciatively elevate PER2 above background in brain and kidney. We have previously shown, at the mRNA level in the brain, that although sleep deprivation generally resulted in levels of *Per2* expression above baseline, these increases were strongly modified by the time of day the sleep deprivation was performed such that mRNA even decreased from their initial levels for sleep

deprivations scheduled between ZT18 and -24.[18] How this interaction between time-of-day and sleep deprivation at the mRNA levels translates into changes in PER2 protein levels is difficult to predict as the temporal relationship between the two seems to differ for circadian and induced aspects of *Per2*–PER2 regulation (see above). Further complicating the interpretation of the sleep deprivation results obtained in arrhythmic SCNx mice is the fact that in the absence of a behavioral phase marker, the timing of the sleep deprivation was determined by that of the sham operated mice. Inspection of the few behaviorally arrhythmic SCNx mice that still showed evidence of circadian rhythmicity in PER2 levels revealed that sleep deprivation was not always performed at the time PER2 decreases as was done for the other experimental groups (data not shown). Whether intact circadian rhythms are a requirement for the sleep-deprivation induced increase in PER2 in the brain can therefore not be conclusively answered here. Future experiments using a recently developed imaging technique for the long-term online monitoring of PER2 bioluminescence in freely behaving mice[40] would enable using the phase of the PER2 rhythm itself (if present), rather than relying on the phase of the activity rhythms to schedule the sleep deprivation. Nevertheless, sleep deprivation did significantly increase PER2 in livers of arrhythmic SCNx mice with dynamics similar to those observed in the other experimental groups demonstrating that at least in this tissue the effects of sleep-deprivation do not depend on a functional circadian clock.

Notwithstanding the limitations of our analysis already mentioned in the results section, we did identify three mice in which circadian rhythms in PER2 were detected while rhythms in locomotor activity were absent after lesioning the SCN. Thus although the SCN is needed for circadian rhythms in overt behaviors, in peripheral organs (including brain areas outside the SCN) molecular circadian rhythms can still be maintained in some cases, consistent with the *ex vivo* experiments performed by Yoo and colleagues[27] and the *in vivo* experiments by us and others[39,40] (but contrasting the work of Guo and colleagues[57]). Importantly, in the two previous studies that did observe circadian PER2 expression in kidney and liver in some of the arrhythmic SCNx mice, it was noted that the amplitudes of the changes in PER2 were reduced. Thus in the intact animal circadian driven behaviors, such as the circadian sleep-wake distribution and the resulting rhythms in e.g. feeding, temperature, metabolism, and clock genes,[2,58,59] contribute to amplify these locally generated rhythms.

Conclusion

Functionally sleep has and still is generally seen as a state needed to ensure proper brain functioning.[51,60,61] It has become clear, however, that sleep loss has immediate adverse consequences on e.g. metabolic balance and immune function (e.g.[62,63]). Accumulating evidence from molecular studies support that altered timing of sleep and sleep loss greatly impact gene expression in the periphery both in mice and humans.[16,24-26] While we see an immediate and profound increase in PER2 in the brain, the effects in liver were longer lasting and preserved in SCNx mice. The liver expression of *Per2* was found to be rhythmic in mice in which the clock circuitry was arrested specifically in liver,[64] demonstrating that rhythms in *Per2* expression can be driven by both systemic cues and peripheral oscillators. In light of our current results the sleep-wake distribution is likely to be one of these systemic cues. Chronic disruption of sleep also affects the peripheral expression of clock genes, including that of *Per2*, in humans.[26] Although chronic sleep loss and disrupted circadian rhythmicity both negatively impact energy metabolism,[62,65-67] whether the same or different pathways are implicated is, however, unknown. Based on our findings that the sleep-wake distribution alters PER2 levels in the periphery, it is tempting to speculate that some of the adverse peripheral effects of sleep loss are mediated through its effects on clock genes.

Acknowledgements

We are greatly indebted to all colleagues who helped with the sleep deprivations (Valérie Hinard, Huyn Hor, Sonja Jimenez, Francesco La Spada, Géraldine Mang, Cyril Mikhail, Valérie Mongrain, Brice Petit, Corinne Pfister, and Julie Vienne). We thank Arnaud Paradis (Cellular Imaging Facility of the University of Lausanne) for help with imaging, Marieke Hoekstra (University of Lausanne) for critical comments on the manuscripts, and David Weaver (University of Massachusetts Medical School) and Ueli Schibler (University of Geneva) for generously providing PER2 antibodies. Research was supported by fellowships of the Marie Curie Intra-European program (IEF-FP7-Project Number: 221254) and the Novartis Foundation to TC, the Swiss National Science Foundation (SNF 31003A-130825, and -146694) to PF, EUMODIC (Contract no.: 037188) supporting YE, the University of Lausanne, and the state of Vaud, Switzerland.

Table and Figure legends

Tissue	LD condition	SCN / behavioral status	% rhythmic PER2 biolum	Sine-wave amplitude [%]	ANOVA 'Time' [*P*]	n
Brain	LD12:12	Intact	100	49.8 (5.3)	<0.0001	13
	DD	Sham	67	40.7 (4.9)	<0.0001	6
		SCNx / rhy	33	22.7 (5.5)	0.0011	6
		SCNx / arr	14	17.0 (2.0)	0.0016	7
Liver	LD12:12	Intact	100	44.3 (3.7)	<0.0001	12
	DD	Sham	86	36.5 (4.7)	<0.0001	7
		SCNx / rhy	75	33.8 (4.4)	<0.0001	8
		SCNx /arr	0	15.9 (1.3)	0.21	5
Kidney	LD12:12	Intact	100	45.1 (2.7)	<0.0001	12
	DD	Sham	57	23.6 (4.6)	<0.0001	7
		SCNx / rhy	13	17.1 (2.5)	<0.0001	8
		SCNx / arr	40	12.7 (3.1)	0.42	5

Table 1: Parameter estimates of PER2 rhythmicity. Rhythmicity of PER2-bioluminescence was assessed by fitting a sine function to the 8 data points measured 3h apart within individual mice with phase and amplitude as free parameters (SAS, proc NLIN). Under light-dark (LD12:12) conditions period was set to 24.0h, while under constant dark (DD) conditions the individual's free-running period of locomotor activity during the recording period was used. Because period length cannot be determined in arrhythmic mice, the mean value of the sham-lesioned mice was used. Individual time courses were deemed rhythmic when the 95% confidence interval estimated for the amplitude of the fitted sine-wave did not cross zero. Note that a sine function could not always be reliably fitted despite clear rhythms in PER2-bioluminescence being present. This was more often the case in the brain where bi-modality of the signal was observed (see Figures 1 and 4). In all tissues the fitted amplitude (including those estimated in mice deemed not rhythmic) was largest in Intact mice under LD12:12 [2-way ANOVA factors 'Group' (Intact, Sham, SCNx/rhy, SCNx/arrhy): $P<0.0001$ and 'Tissue' (Brain, Liver, Kidney): $P=0.015$; interaction: $P=0.28$; Brain: Intact > SCNx/rhy, SCNx/arrhy; Sham > SCNx/arrhy; Liver: SCNx/arrhy < Intact, Sham, SCNx/rhy; Kidney: Intact > Sham, SCNx/rhy, SCNx/arrhy; post-hoc Tukey, $P<0.05$). Finally, ANOVA analyses revealed that in all 3 tissues of the Intact, Sham, and SCNx/rhythmic groups the effects of factor 'Time' was significant, while in the SCNx/arrhythmic group only in the brain a significant time effect was observed. Note that this ANOVA analyses does not test for the presence of circadian rhythmicity and that in the SCNx/arrhythmic group the time course of bioluminescence could not be objectively aligned among

individuals because phase-markers of circadian rhythmicity were lacking. For this group, phase and period to align data were taken from the Sham group averages that were recorded in parallel.

Figure 1: Time-of-day and sleep deprivation affect PER2 protein levels under light-dark conditions. **A**: An example of the daily changes (ZT0-24; 3h intervals) in bioluminescence (color coded as 'heat' scores) emanating from the left frontal cerebral cortex through a glass cylinder (red arrow in left panel) of an individual of *Per2*^{Luc} mice. Bioluminescence images are superimposed on photos of the mouse's head. Luciferin was delivered through a cannula (yellow arrow) into the right lateral ventricle. Strongest signals (red color) were observed at ZT21 and ZT0/24. **B**: Mean (±1 SEM) bioluminescence levels in brain, liver, and kidney (n=12) under baseline conditions (ZT0-24; 3h intervals; grey line) and at ZT6, -8, and -12 (black line) after a 6h sleep deprivation (SD; ZT0-6; dashed line). Values were expressed as % of the individual mean bioluminescence in baseline before averaging. Horizontal dashed lines indicate mean bioluminescence (i.e., 100%). Blue data point indicates mean (±1 SEM) bioluminescence at ZT3 after a 3h SD (n=3). **C**: Mean fold-change in bioluminescence (vertical bars, +1 SE of the ratio) in brain (black), liver (brown), and kidney (green bars) at 0-, 2-, and 6h of recovery after SD (i.e., ZT6, -8, and -12) compared to corresponding baseline measures within individuals. Red triangles mark significant deviations from baseline (post-hoc paired t-tests; $P<0.05$). The initial increase after SD, at ZT6, is larger in brain compared to kidney (red asterisk; post-hoc Tukey; $P<0.05$). **D:** Time course of mean locomotor activity. Hourly values were expressed as % of the mean individual 24h activity before averaging. Horizontal line indicates mean activity (i.e., 100%). Grey areas in panels B and D delineate the 12h dark periods.

Figure 2: Brain immunohistofluorescence of PER2 after a 6h sleep deprivation. **A**: Representative examples of sagittal brain sections of *Per2*^{Luc} mice showing PER2 expression (green pseudocolor) at ZT6 under baseline conditions (CTRL) and after a 6h sleep deprivation (SD; ZT0-6). In addition, sections were stained for AVP (red), to mark the SCN, and DAPI (blue), to visualize cell nuclei. White boxed areas mark the five brain regions detailed in Panels **B**-**E**; i.e., cerebral cortex (**B**), SCN (**C**), cerebellum (**D**), and the hippocampal areas *Cornu Ammonis* (CA; **E**) and dendate gyrus (DG, **F)**. Roman numerals in panel B indicate cortical layers I-VI with tick marks estimating layer boundaries based on visual inspection of cyto-architectural variation in each section. Scale bar in panel A is 1250µm and in panels B-F 50µm.

Figure 3: Brain immunohistofluorescence of PER2 as a function of time-of-day. **A**: Sagittal brain sections of *Per2*^{Luc} mice showing PER2 levels (green) co-stained with an AVP antibody (red; lower 4 panels) at ZT0, -6, -12, and -18. Note the red AVP staining in the SCN (box C) turning yellow when PER2 is high (ZT12 and -18). The same sections were counterstained for DAPI (blue; upper 4 panels). Detailed PER2 staining is shown for cerebral cortex (**B**), SCN (**C**), cerebellum (**D**), and the *Cornu Ammonis* (CA) (**E**) and dendate gyrus (DG, **F**). Details for SCN (C), cerebellum (D), and CA (E) shown at higher magnification at times of high PER2 expression (i.e., ZT12, -18, and -18, respectively). Note that 1) many PER2 positive cells can be seen in cortical layers IV and V, 2) most PER2 positive cells (green) in the SCN also express AVP (red; yellow when overlain), 3) the cytoplasm and axons but not the nuclei of Purkinje neurons in the cerebellum express PER2 (see white arrows), and 4) many cells in the hippocampus, specifically in the granule cell layer and subgranular zone, are PER2 positive. **G**: Quantification of PER2 fluorescence for the five brain regions at ZT0 (double plotted at ZT24), -6, -12, and -18 (gray line) and at ZT6 after a 6h sleep deprivation (SD; ZT0-6; black line; see data in Figure 2). Numbers besides data points indicate other ZT times from which the data point significantly differed (post-hoc Tukey; $P<0.05$). Note that SD significantly changed PER2 levels only in the cerebral cortex (red asterisk; post-hoc t-test; $P<0.05$). Grey areas mark the 12h dark periods. Scale bar in panel A is 1250µm, in panels B-E and in details 50µm. See Figure 2 for details.

Figure 4: PER2 bioluminescence levels as a function of circadian time in sham operated mice and in rhythmic and arrhythmic SCN-lesioned mice under constant dark conditions. **A**: Mean (±1 SEM) bioluminescence levels in brain, liver, and kidney under baseline conditions (CT0-24; 3h intervals; grey line; for n/group/tissue see Table 1). Values were expressed as percentage of individual mean bioluminescence in baseline before averaging. CT within individuals was calculated according the individual's free-running period using activity onset as CT12 for the sham and SCNx/rhythmic *Per2*^{Luc} mice (see Panel B). For SCNx/arrhythmic mice mean period and activity onset of the sham group were used to construct an average time course. **B**: Mean circadian locomotor activity waveforms for sham lesioned and SCNx-rhythmic and -arrhythmic mice. Activity values were expressed as a percentage of each individual's mean activity. Note the two peaks in the activity for Sham and SCNx/ rhythmic mice. Grey and white areas delineate the subjective dark or active (α) and light or rest (ρ) periods, respectively.

Figure 5: **PER2 levels after sleep deprivation in sham operated mice and in rhythmic and arrhythmic SCN-lesioned mice under constant dark conditions. A.** Mean (±1 SEM) bioluminescence levels in brain, liver, and kidney under baseline conditions (CT0, -6, -8, and -12; grey line), and after 0-, 2-, and 6h of recovery sleep following a 6h sleep deprivation (SD CT0-6, dashed line, black line;

brain: n=3, 4, and 4; liver and kidney: n=3, 3, and 5 for sham, SCNx-rhythmic, and -arrhythmic mice, respectively). PER2 values were expressed as a percentage of the individual mean bioluminescence in baseline. As the 4 baseline measurements obtained in these mice did not span an entire cycle direct comparisons to the relative values depicted in Figures 1 and 4 could not be made. To accommodate this we linearly adjusted the average values obtained here to the 4 corresponding mean relative baseline values depicted in Figure 4. Grey areas delineate subjective dark periods; i.e., α. **B.** Mean fold-change in bioluminescence (vertical bars, +1 SE of the ratio) in brain (black), liver (brown), and kidney (green bars) after 6h SD compared to their own corresponding baseline. Red triangles mark significant deviations from baseline (post-hoc paired t-tests; $P<0.05$).

References:

1. Dijk DJ, Franken P. Interaction of Sleep Homeostasis and Circadian Rhythmicity: Dependent or Independent Systems? In: Meir H. Kryger MH, Roth T., Dement W., ed. Principles and practice of sleep medecine. 4th edition ed: Saunders/Elsevier, 2005.
2. Franken P. A role for clock genes in sleep homeostasis. Curr Opin Neurobiol 2013;23(5):864-72.
3. Franken P, Lopez-Molina L, Marcacci L, Schibler U, Tafti M. The transcription factor DBP affects circadian sleep consolidation and rhythmic EEG activity. J Neurosci 2000;20(2):617-25.
4. Hendricks JC, Lu S, Kume K, Yin JC, Yang Z, Sehgal A. Gender dimorphism in the role of cycle (BMAL1) in rest, rest regulation, and longevity in Drosophila melanogaster. Journal of Biological Rhythms 2003;18(1):12-25.
5. Kopp C, Albrecht U, Zheng B, Tobler I. Homeostatic sleep regulation is preserved in mPer1 and mPer2 mutant mice. Eur J Neurosci 2002;16(6):1099-106.
6. Naylor E, Bergmann BM, Krauski K, et al. The circadian clock mutation alters sleep homeostasis in the mouse. J Neurosci 2000;20(21):8138-43.
7. Shaw PJ, Tononi G, Greenspan RJ, Robinson DF. Stress response genes protect against lethal effects of sleep deprivation in Drosophila. Nature 2002;417(6886):287-91.
8. Wisor JP, O'Hara BF, Terao A, et al. A role for cryptochromes in sleep regulation. BMC Neurosci 2002;3:20.
9. Laposky A, Easton A, Dugovic C, Walisser J, Bradfield C, Turek F. Deletion of the mammalian circadian clock gene BMAL1/Mop3 alters baseline sleep architecture and the response to sleep deprivation. Sleep 2005;28(4):395-409.
10. Franken P, Dudley CA, Estill SJ, et al. NPAS2 as a transcriptional regulator of non-rapid eye movement sleep: genotype and sex interactions. Proc Natl Acad Sci U S A 2006;103(18):7118-23.
11. He Y, Jones CR, Fujiki N, et al. The transcriptional repressor DEC2 regulates sleep length in mammals. Science 2009;325(5942):866-70.
12. Viola AU, Archer SN, James LM, et al. PER3 polymorphism predicts sleep structure and waking performance. Current Biology 2007;17(7):613-8.
13. Mang GM, Franken P. Genetic Dissection of Sleep Homeostasis. Curr Top Behav Neurosci 2013.
14. Mongrain V, La Spada F, Curie T, Franken P. Sleep loss reduces the DNA-binding of BMAL1, CLOCK, and NPAS2 to specific clock genes in the mouse cerebral cortex. PloS ONE 2011;6(10):e26622.
15. Franken P, Thomason R, Heller HC, O'Hara BF. A non-circadian role for clock-genes in sleep homeostasis: a strain comparison. BMC Neurosci 2007;8:87.

16. Maret S, Dorsaz S, Gurcel L, et al. Homer1a is a core brain molecular correlate of sleep loss. Proc Natl Acad Sci U S A 2007;104(50):20090-5.
17. Mongrain V, Hernandez SA, Pradervand S, et al. Separating the contribution of glucocorticoids and wakefulness to the molecular and electrophysiological correlates of sleep homeostasis. Sleep 2010;33(9):1147-57.
18. Curie T, Mongrain V, Dorsaz S, Mang GM, Emmenegger Y, Franken P. Homeostatic and circadian contribution to EEG and molecular state variables of sleep regulation. Sleep 2013;36(3):311-23.
19. Reppert SM, Weaver DR. Molecular analysis of mammalian circadian rhythms. Annu Rev Physiol 2001;63:647-76.
20. Nishii K, Yamanaka I, Yasuda M, et al. Rhythmic post-transcriptional regulation of the circadian clock protein mPER2 in mammalian cells: a real-time analysis. Neuroscience Letters 2006;401(1-2):44-8.
21. Tamanini F, Yagita K, Okamura H, van der Horst GT. Nucleocytoplasmic shuttling of clock proteins. Methods in enzymology 2005;393:418-35.
22. Franken P, Malafosse A, Tafti M. Genetic determinants of sleep regulation in inbred mice. Sleep 1999;22(2):155-69.
23. Franken P, Chollet D, Tafti M. The Homeostatic Regulation of Sleep Need Is under Genetic Control. J. Neurosci. 2001;21(8):2610-21.
24. Barclay JL, Husse J, Bode B, et al. Circadian desynchrony promotes metabolic disruption in a mouse model of shiftwork. PLoS One 2012;7(5):e37150.
25. Anafi RC, Pellegrino R, Shockley KR, Romer M, Tufik S, Pack AI. Sleep is not just for the brain: transcriptional responses to sleep in peripheral tissues. BMC genomics 2013;14:362.
26. Moller-Levet CS, Archer SN, Bucca G, et al. Effects of insufficient sleep on circadian rhythmicity and expression amplitude of the human blood transcriptome. Proc Natl Acad Sci U S A 2013;110(12):E1132-41.
27. Yoo SH, Yamazaki S, Lowrey PL, et al. PERIOD2::LUCIFERASE real-time reporting of circadian dynamics reveals persistent circadian oscillations in mouse peripheral tissues. Proc Natl Acad Sci U S A 2004;101(15):5339-46.
28. Franken P, Dijk DJ, Tobler I, Borbely AA. Sleep deprivation in rats: effects on EEG power spectra, vigilance states, and cortical temperature. Am J Physiol 1991;261(1 Pt 2):R198-208.
29. Abraham U, Prior JL, Granados-Fuentes D, Piwnica-Worms DR, Herzog ED. Independent circadian oscillations of Period1 in specific brain areas in vivo and in vitro. J Neurosci 2005;25(38):8620-6.
30. Franken P, Dijk DJ. Circadian clock genes and sleep homeostasis. Eur J Neurosci 2009;29(9):1820-9.
31. Reppert SM, Weaver DR. Coordination of circadian timing in mammals. Nature 2002;418(6901):935-41.
32. Antle MC, Mistlberger RE. Circadian clock resetting by sleep deprivation without exercise in the Syrian hamster. J Neurosci 2000;20(24):9326-32.
33. Deboer T, Detari L, Meijer JH. Long term effects of sleep deprivation on the mammalian circadian pacemaker. Sleep 2007;30(3):257-62.
34. Millar AJ, Short SR, Chua NH, Kay SA. A novel circadian phenotype based on firefly luciferase expression in transgenic plants. The Plant cell 1992;4(9):1075-87.
35. Kondo T, Strayer CA, Kulkarni RD, et al. Circadian rhythms in prokaryotes: luciferase as a reporter of circadian gene expression in cyanobacteria. Proc Natl Acad Sci U S A 1993;90(12):5672-6.
36. Welsh DK, Yoo SH, Liu AC, Takahashi JS, Kay SA. Bioluminescence imaging of individual fibroblasts reveals persistent, independently phased circadian rhythms of clock gene expression. Current Biology 2004;14(24):2289-95.

37. Nagoshi E, Saini C, Bauer C, Laroche T, Naef F, Schibler U. Circadian gene expression in individual fibroblasts: cell-autonomous and self-sustained oscillators pass time to daughter cells. Cell 2004;119(5):693-705.
38. Yamaguchi S, Kobayashi M, Mitsui S, et al. View of a mouse clock gene ticking. Nature 2001;409(6821):684.
39. Tahara Y, Kuroda H, Saito K, et al. In vivo monitoring of peripheral circadian clocks in the mouse. Current Biology 2012;22(11):1029-34.
40. Saini C, Liani A, Curie T, et al. Real-time recording of circadian liver gene expression in freely moving mice reveals the phase-setting behavior of hepatocyte clocks. Genes Dev 2013;27(13):1526-36.
41. Yan L, Silver R. Resetting the brain clock: time course and localization of mPER1 and mPER2 protein expression in suprachiasmatic nuclei during phase shifts. Eur J Neurosci 2004;19(4):1105-9.
42. Mateju K, Bendova Z, El-Hennamy R, Sladek M, Sosniyenko S, Sumova A. Development of the light sensitivity of the clock genes Period1 and Period2, and immediate-early gene c-fos within the rat suprachiasmatic nucleus. Eur J Neurosci 2009;29(3):490-501.
43. Segall LA, Amir S. Exogenous corticosterone induces the expression of the clock protein, PERIOD2, in the oval nucleus of the bed nucleus of the stria terminalis and the central nucleus of the amygdala of adrenalectomized and intact rats. J Mol Neurosci 2010;42(2):176-82.
44. Noback CRR, D. A.; Demarest, R. J.; Strominger, N. L. The Human Nervous System: Structure and Function: Humana Press, 2005.
45. Masubuchi S, Honma S, Abe H, et al. Clock genes outside the suprachiasmatic nucleus involved in manifestation of locomotor activity rhythm in rats. Eur J Neurosci 2000;12(12):4206-14.
46. Wakamatsu H, Yoshinobu Y, Aida R, Moriya T, Akiyama M, Shibata S. Restricted-feeding-induced anticipatory activity rhythm is associated with a phase-shift of the expression of mPer1 and mPer2 mRNA in the cerebral cortex and hippocampus but not in the suprachiasmatic nucleus of mice. Eur J Neurosci 2001;13(6):1190-6.
47. Pezuk P, Mohawk JA, Yoshikawa T, Sellix MT, Menaker M. Circadian organization is governed by extra-SCN pacemakers. Journal of Biological Rhythms 2010;25(6):432-41.
48. Abe H, Honma S, Namihira M, Masubuchi S, Honma K. Behavioural rhythm splitting in the CS mouse is related to clock gene expression outside the suprachiasmatic nucleus. Eur J Neurosci 2001;14(7):1121-8.
49. Dudley CA, Erbel-Sieler C, Estill SJ, et al. Altered patterns of sleep and behavioral adaptability in NPAS2-deficient mice. Science 2003;301(5631):379-83.
50. Tu BP, McKnight SL. Metabolic cycles as an underlying basis of biological oscillations. Nat Rev Mol Cell Biol 2006;7(9):696-701.
51. Krueger JM, Rector DM, Roy S, Van Dongen HP, Belenky G, Panksepp J. Sleep as a fundamental property of neuronal assemblies. Nat Rev Neurosci 2008;9(12):910-9.
52. Jones BE. Arousal systems. Front Biosci 2003;8:s438-51.
53. Borgs L, Beukelaers P, Vandenbosch R, et al. Period 2 regulates neural stem/progenitor cell proliferation in the adult hippocampus. BMC Neurosci 2009;10:30.
54. Shieh KR, Yang SC, Lu XY, Akil H, Watson SJ. Diurnal rhythmic expression of the rhythm-related genes, rPeriod1, rPeriod2, and rClock, in the rat brain. Journal of biomedical science 2005;12(1):209-17.
55. Mendoza J, Pevet P, Felder-Schmittbuhl MP, Bailly Y, Challet E. The cerebellum harbors a circadian oscillator involved in food anticipation. J Neurosci 2010;30(5):1894-904.
56. Rath MF, Rovsing L, Moller M. Circadian oscillators in the mouse brain: molecular clock components in the neocortex and cerebellar cortex. Cell Tissue Res 2014;357(3):743-55.
57. Guo H, Brewer JM, Champhekar A, Harris RB, Bittman EL. Differential control of peripheral circadian rhythms by suprachiasmatic-dependent neural signals. Proceedings of the National Academy of Sciences of the United States of America 2005;102(8):3111-6.

58. Franken P, Tobler I, Borbely AA. Sleep and waking have a major effect on the 24-hr rhythm of cortical temperature in the rat. Journal of Biological Rhythms 1992;7(4):341-52.
59. Maquet P. Sleep function(s) and cerebral metabolism. Behavioural Brain Research 1995;69(1-2):75-83.
60. Hobson JA. Sleep is of the brain, by the brain and for the brain. Nature 2005;437(7063):1254-6.
61. Tononi G, Cirelli C. Sleep function and synaptic homeostasis. Sleep Med Rev 2006;10(1):49-62.
62. Spiegel K, Tasali E, Leproult R, Van Cauter E. Effects of poor and short sleep on glucose metabolism and obesity risk. Nat Rev Endocrinol 2009;5(5):253-61.
63. Besedovsky L, Lange T, Born J. Sleep and immune function. Pflugers Arch 2012;463(1):121-37.
64. Kornmann B, Schaad O, Bujard H, Takahashi JS, Schibler U. System-driven and oscillator-dependent circadian transcription in mice with a conditionally active liver clock. PLoS Biol 2007;5(2):e34.
65. Bass J, Takahashi JS. Circadian integration of metabolism and energetics. Science 2010;330(6009):1349-54.
66. Sadacca LA, Lamia KA, deLemos AS, Blum B, Weitz CJ. An intrinsic circadian clock of the pancreas is required for normal insulin release and glucose homeostasis in mice. Diabetologia 2011;54(1):120-4.
67. Zani F, Breasson L, Becattini B, et al. PER2 promotes glucose storage to liver glycogen during feeding and acute fasting by inducing Gys2 PTG and G L expression. Molecular metabolism 2013;2(3):292-305.

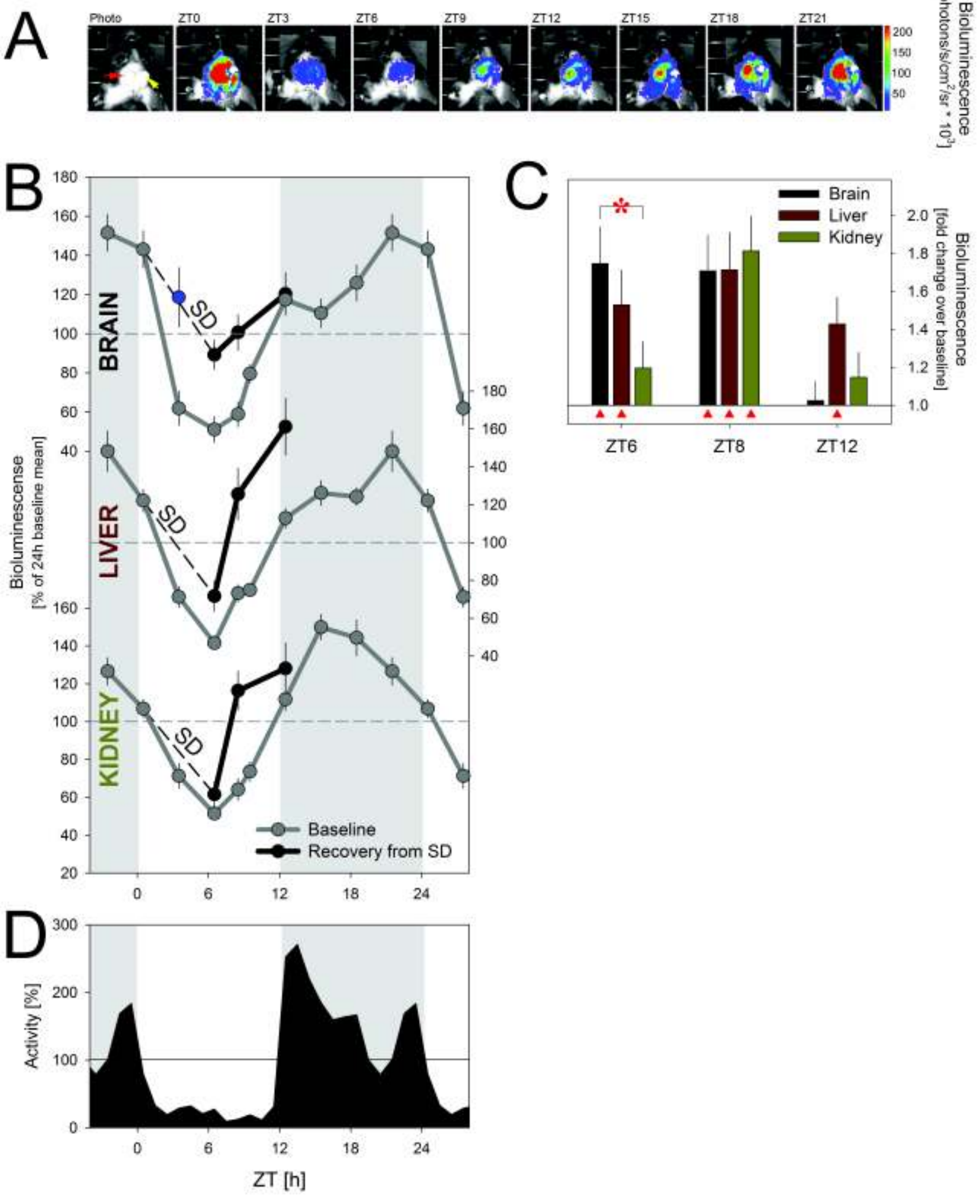
A
Photo
ZT0
ZT3
ZT6
ZT9
ZT12
ZT15
ZT18
ZT21
200
150
100
50
Bioluminescence
[photons/s/cm²/sr * 10³]
B
BRAIN
LIVER
KIDNEY
SD
Baseline
Recovery from SD
Bioluminescense
[% of 24h baseline mean]
ZT [h]
C
Brain
Liver
Kidney
Bioluminescence
[fold change over baseline]
ZT6
ZT8
ZT12
D
Activity [%]
ZT [h]

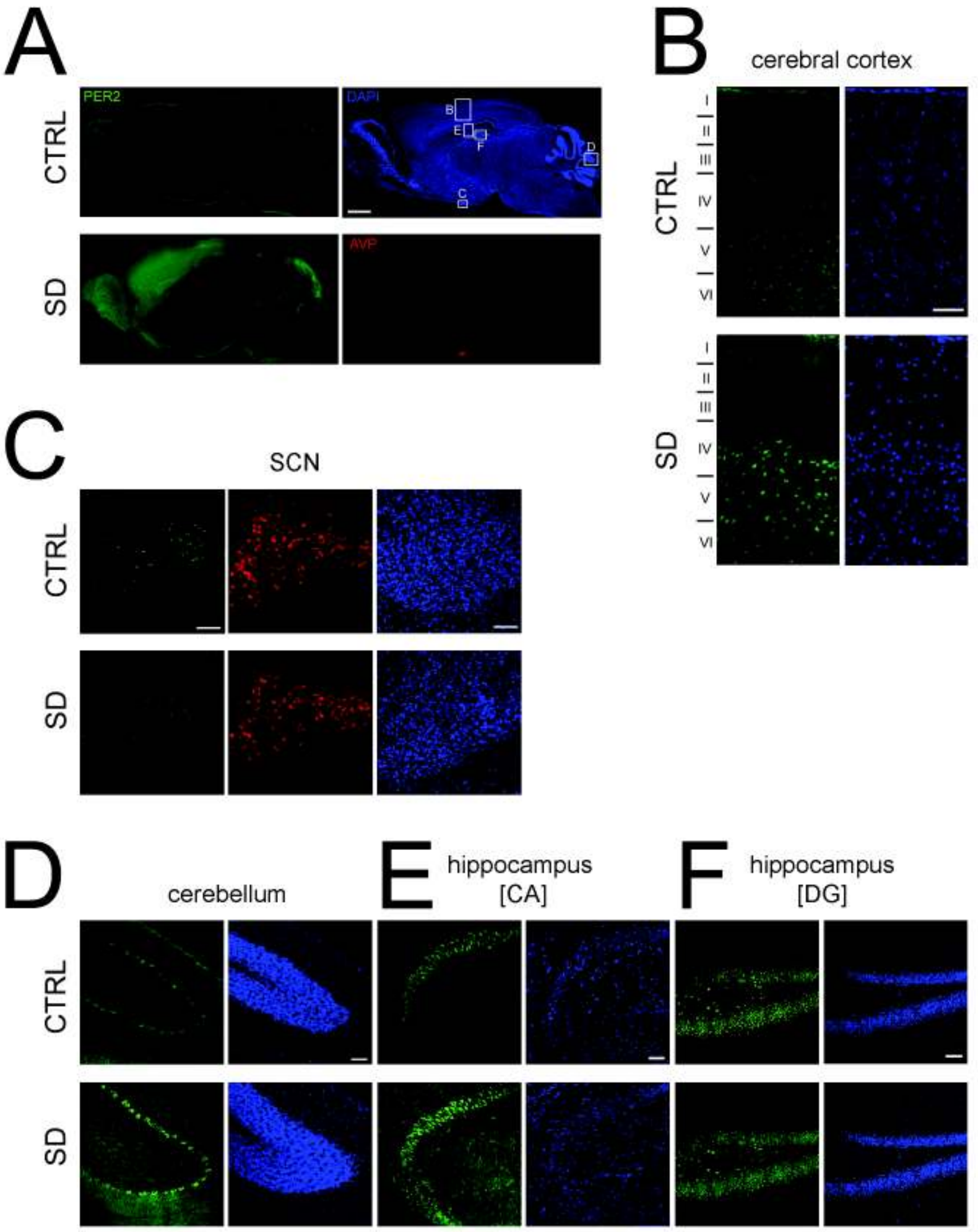
A
PER2
DAPI
B
E
F
D
C
CTRL
SD
AVP
B
cerebral cortex
CTRL
SD
I
II
III
IV
V
VI
C
SCN
CTRL
SD
D
cerebellum
E
hippocampus
[CA]
F
hippocampus
[DG]
CTRL
SD

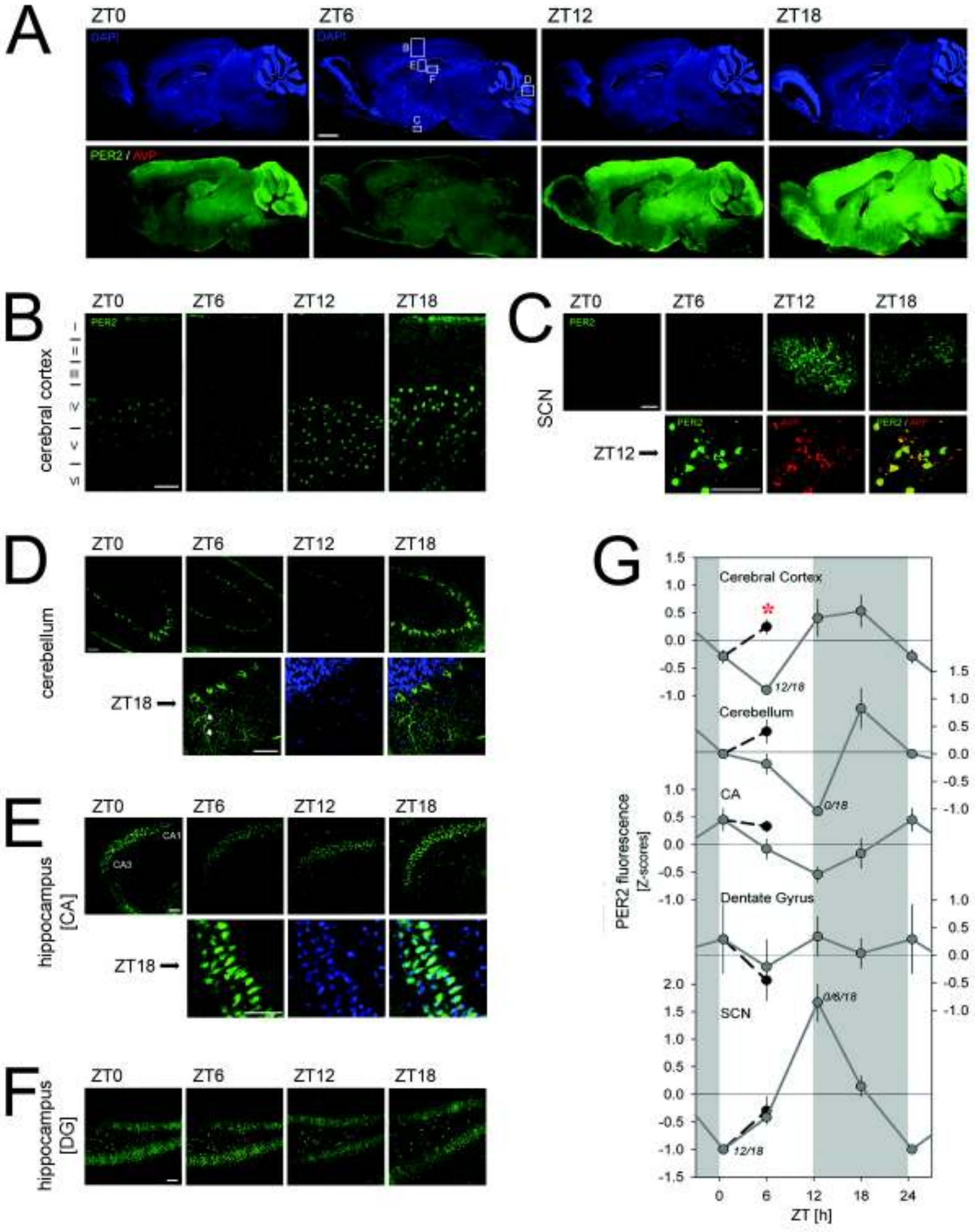
A
ZT0
ZT6
ZT12
ZT18
DAPI
PER2 / AVP
B
cerebral cortex
PER2
C
SCN
ZT12
D
cerebellum
ZT18
E
hippocampus [CA]
CA1
CA3
F
hippocampus [DG]
G
Cerebral Cortex
Cerebellum
CA
Dentate Gyrus
SCN
12/18
0/18
0/6/18
PER2 fluorescence [Z-scores]
ZT [h]

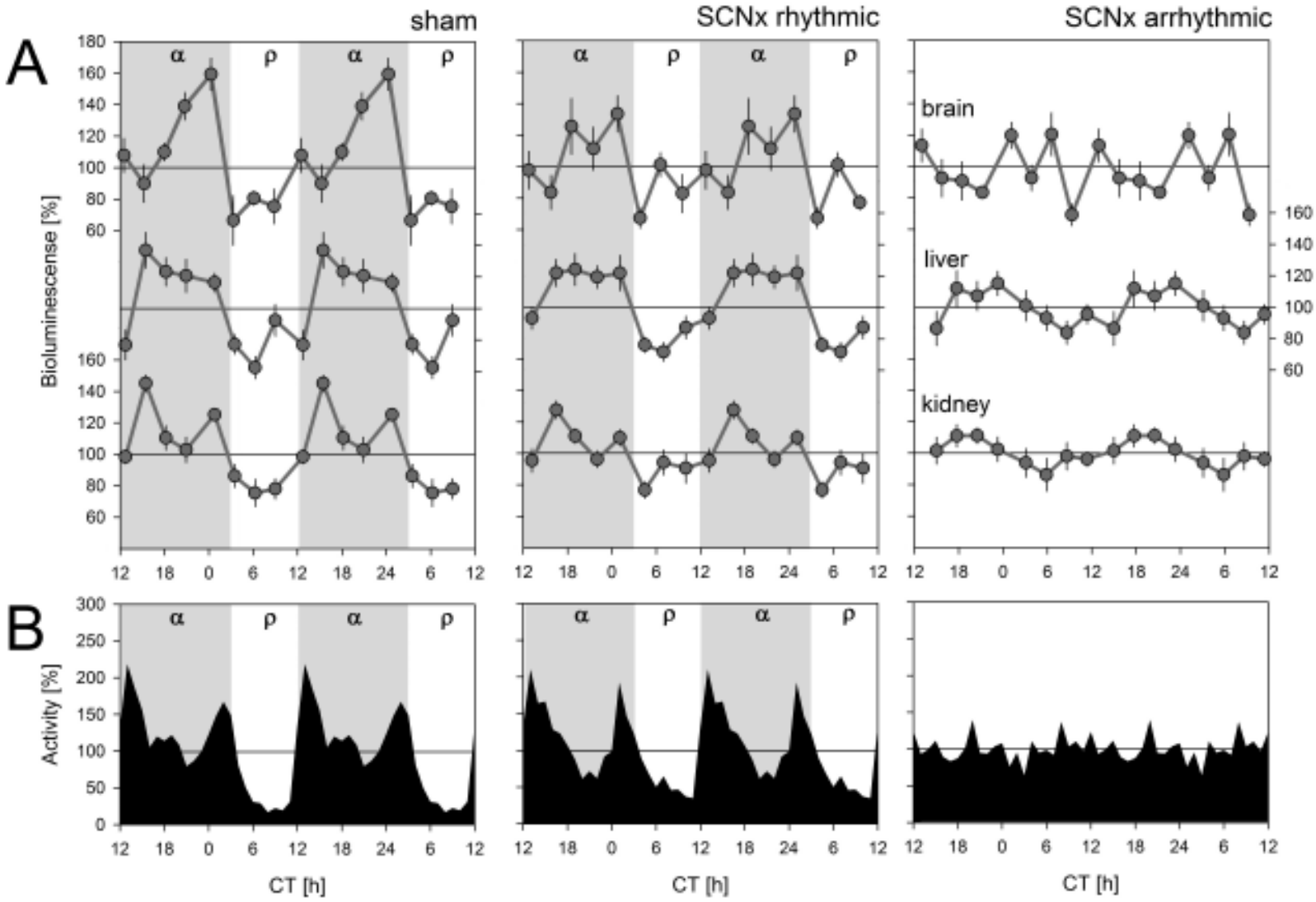
A
sham
SCNx rhythmic
SCNx arrhythmic
α
ρ
brain
liver
kidney
Bioluminescense [%]
B
Activity [%]
CT [h]

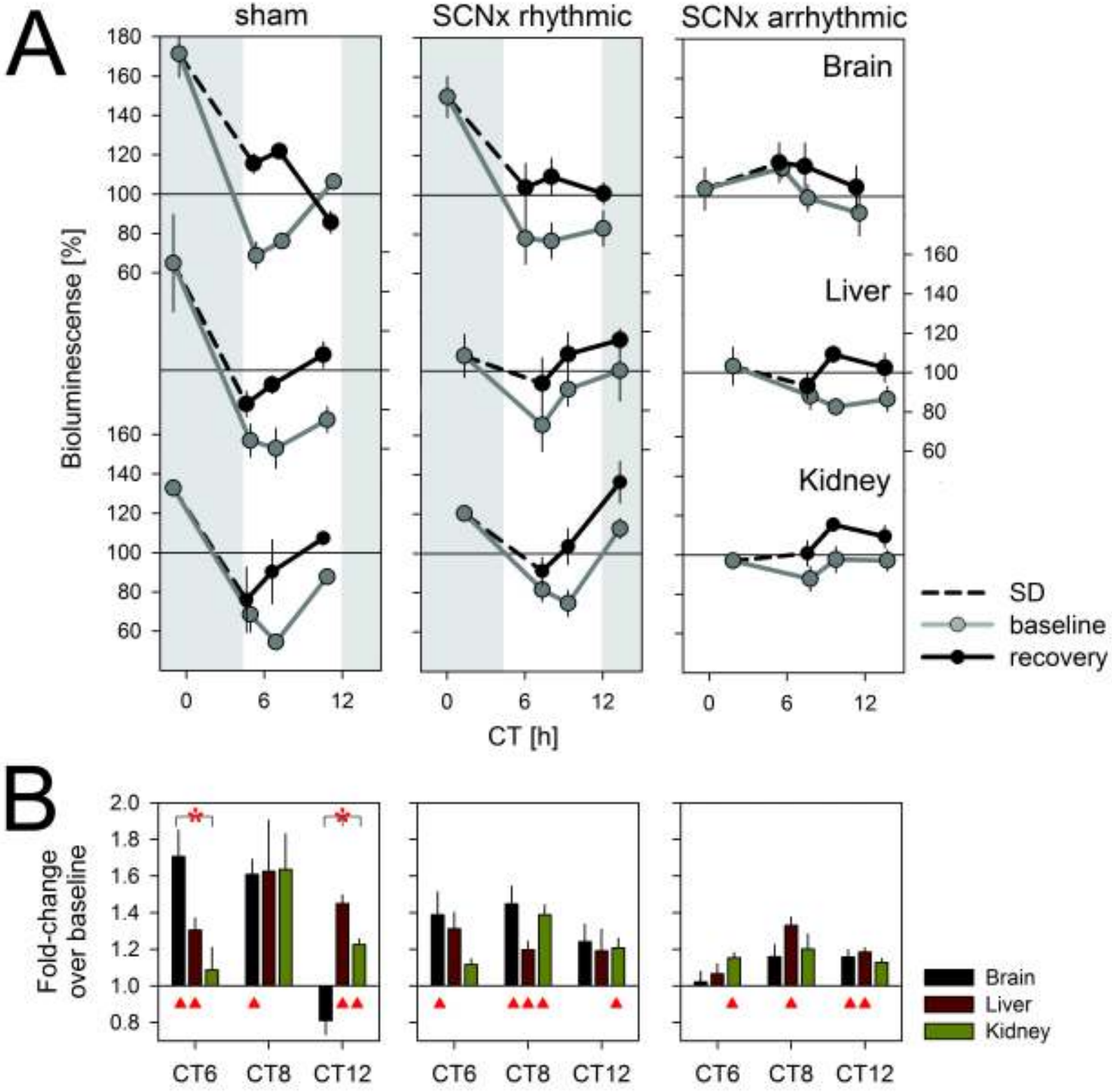
A
sham
SCNx rhythmic
SCNx arrhythmic
Brain
Liver
Kidney
Bioluminescense [%]
CT [h]
SD
baseline
recovery
B
Fold-change over baseline
CT6
CT8
CT12
Brain
Liver
Kidney

Supplemental Information

"In vivo imaging of the central and peripheral effects of sleep deprivation and SCN lesion on PERIOD-2 protein in mice" by Curie, Maret, Emmenegger, and Franken

1. Inventory of Supplemental Information

As supplemental information we provide three experimental procedures, concerning the EEG recordings, Western-blot analyses, and 3D bioluminescence reconstruction, respectively, and 5 figures: Figure S1 shows sleep EEG recordings in *Per2*^{Luc} mice under baseline and sleep deprivation conditions. Figure S2 illustrates the 3D reconstruction of bioluminescence source localization of peripheral PER2 protein. Figure S3 illustrates the protocol used to sample bioluminescence in living *Per2*^{Luc} mice and locomotor activity data demonstrating that circadian rhythms in *Per2*^{Luc} knock-in mice are not compromised by the knock-in construct. Figure S4 presents PER2 western-blot analyses supporting the bioluminescence data in main Figure 1. Figure S5 shows rhythmicity in intact, sham, rhythmic, and arrhythmic SCN-lesioned *Per2*^{Luc} mice with Nissl staining confirming the presence or absence of SCN.

2. Supplemental Experimental Procedures

Experimental Procedure 1: EEG recording and analysis in *Per2*^{Luc} mice.

Electroencephalogram and Electromyogram (EEG/EMG) surgeries were performed according to the methods described previously[1] with minor changes. Briefly, EEG and EMG electrodes were implanted under deep ketamine/xylazine anesthesia (intraperitoneal injection, 75- and 10mg/kg, at a volume of 8ml/kg). Two gold-plated screws (diameter 1.1mm) served as EEG electrodes and were screwed into the skull over the right cerebral hemisphere (frontal: 1.7mm lateral to midline, 1.5mm anterior to bregma; parietal 1.7mm lateral to midline, 1.0mm anterior to lambda). Four additional screws were used as anchor screws. Two semi-rigid gold wires were used for EMG electrodes and were inserted into the neck musculature along the back of the skull. The four electrodes were soldered to a connector and cemented to the skull. After recovery from surgery (4-7 days) mice were connected to a swivel contact through recording leads to which they could habituate for 7 days prior to the experiment.

Per2^{Luc} mice (n=6 males, 3 months old), were recorded for 96 continuous hours of which the first 48h served as baseline followed by 6h of SD and recovery. EEG and EMG signals were amplified, filtered, and analogy-to-digital converted (200Hz). The behavioral states wakefulness

(W), rapid eye movement sleep (REMS), and non-REM sleep (NREMS) were visually assigned for consecutive 4s epochs as described previously.[1] EEG signals were subjected to a discrete Fourier transform (DFT) to determine EEG power density in the delta frequency range (i.e., delta power, 1-4Hz) for 4s epochs scored as NREMS. Differences in absolute levels of delta power among individuals were accounted for by expressing it as a percentage of the mean delta power over the last 4h of the two baseline light periods. Delta power was averaged for 12 intervals to which an equal number of NREMS epochs contributed (i.e., percentiles) during the 12h light periods, for 6 intervals during the 12h dark periods, and for 8 intervals during the 6h immediately following SD (recovery). Choice of the number of percentiles per recording segment depended on the amount of NREMS present.

Experimental Procedure 2: Western-blot analyses

To assess changes in PER2 protein levels in brain and liver, mice were sleep deprived (ZT0-6) and then sacrificed together with their home-cage controls by cervical dislocation at ZT6, -8, and -12. Baseline levels were assessed also at ZT0 and -18 [males, 3-month old, n=2 and 3 / time point in B6 and homozygote *mPer2*^{Luc} mice, respectively; total n=40). Liver and brain tissues were dissected and frozen immediately on dry ice. Then, tissues were homogenized at 4°C for 30min in RIPA lysis buffer (Tris-HCl 50mM pH7.4; NaCl 150mM; EDTA 1mM; NP-40; Na-deoxycholate 10%; and one complete mini protease inhibitor mixture tablet for 50ml, Roche) and homogenates were cleared by centrifugation for 10min at 13'000rpm and 4°C. Protein concentration was calculated using the bicinchoninic acid assay (Pierce, Rockford, IL, USA) with BSA as a reference. 100 µg of protein were then mixed with an equal volume of loading buffer (glycerol 20%; SDS4%; Tris 100mM; β-mercaptoethanol 5%; and bromophenol blue) before being heated to 98°C for 5min. Proteins were loaded on 8% SDS-polyacrylamide gel electrophoresis and transferred on a nitrocellulose membrane (Millipore) in transfer buffer (Glycine 192mM, Tris 25mM and methanol 20%).

Membranes were then incubated with anti-mPER2 antibodies overnight at 4°C (for liver: rabbit anti-mPER2, 1:1000, generously provided by David Weaver, University of Massachusetts Medical School; for brain: rabbit anti-mPER2, 1:5000; generously provided by Ueli Schibler, University of Geneva). After washing, membranes were incubated with peroxidase-conjugated secondary anti-rabbit antibody (1:10000; Promega) 2h at RT. Blots were then developed using chemoluminescence ECL substrate (Amersham Life Science, Piscataway, NJ, USA). Membranes

were stripped with Restore™ blot stripping buffer (Pierce), washed and incubated one night at 4°C with rabbit polyclonal anti-tubulin (1:5000; Abcam, Cambridge, MA, USA) used as internal control. Quantification of the bands was carried out by densitometric analysis using ImageJ 1.33u software.

Experimental Procedure 3: 3D-reconstruction of bioluminescence source localization

The source of bioluminescence from peripheral organs was localized using 3D-reconstruction (Living Image 3.0 software; Xenogen) (see Figure S2). *Per2*^{Luc} mice (males, 3 months of age, n=4) were shaved completely. 3D reconstruction of the bioluminescence source was achieved by multiple images taken at 45°-increments around the mouse. At each angle three readings were made with long-pass filters set at λ=570-, 600-, and 660nm, respectively, followed by a structured light image to determine the 3D surface topography of each animal. With this information the Diffuse Luminescence Imaging Tomography (DLIT) algorithm (Igor image analysis software, Wavemetrics), which models photon transport in tissue, can localize photon source. For each view, surface topography is determined from phase shifts of parallel line patterns; i.e., structured light projected onto the surface. The partial surface meshes are then stitched together to produce a whole-animal surface mesh. This experiment was performed at ZT18 when PER2 protein expression in the periphery has been shown to be the highest.[2]

3. Supplemental Figures

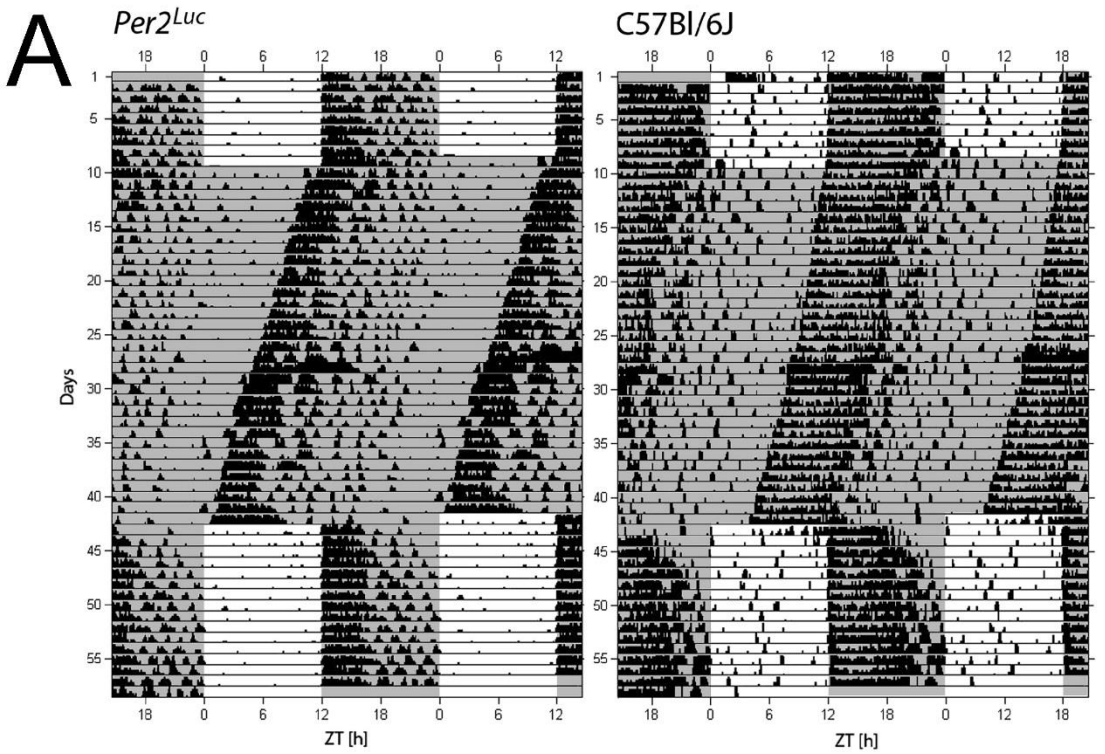

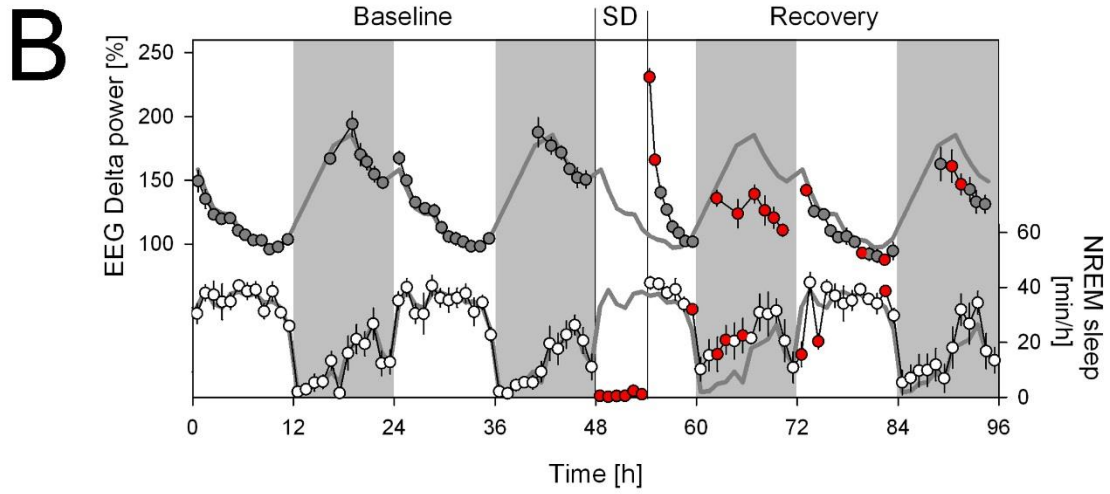

Figure S1: Circadian locomotor activity rhythms and sleep regulation in *Per2*^{Luc} mice. **A**) Two double-plotted actograms of one *Per2*^{Luc} (left) and one wild-type (right) male mice to illustrate that the *Per2*^{Luc} construct does not impact activity profiles both under LD12:12 and DD conditions. Dark periods shown in grey. Activity recorded with passive infrared (PIR) sensors. The *Per2*^{Luc} genetic background is C57Bl/6J. **B**) Mean (±1SEM) time course of EEG delta power during non rapid-eye-movement (NREM) sleep (left y-axis, upper graph) and time spent in NREM sleep (right y-axis, lower graph) recorded for 48h baseline (hours 0-48), 6h sleep deprivation (SD; ZT0-6; hours 48-54), and 42h recovery (hours 54-96). EEG delta power was expressed as a % of the last 4h of the two baseline light periods to correct for inter-individual difference in EEG amplitude and is depicted by grey circles connected by thin black lines. Time spent in NREM sleep was calculated in minutes per recording hour and depicted by open circles connected by thin black lines. Thicker grey lines represent the mean time course over the 2 baselines re-plotted for each of the 4 recording days facilitating the visual assessment of recovery-baseline differences. Grey areas delineate the 12h dark periods. Red filled symbols mark intervals for which SD and recovery values significantly deviated from corresponding baseline values (post-hoc, paired t-test, $P<0.05$). Since only very little NREM sleep was present during the SD, meaningful levels of EEG delta power during this state could not be determined during this period. EEG delta power quantifies the prevalence and amplitude of EEG delta oscillations (1-4 Hz) characteristic of NREM sleep. EEG delta power is in a quantitative and predictive relationship with time-spent-awake and asleep such that during NREM sleep following prolonged periods wakefulness (including SD) EEG delta power is high while during times when NREM sleep prevails, it decreases. For this reason EEG delta power has been widely used as a measure of homeostatic sleep need and sleep depth. Dynamics of EEG delta power and time spent in NREM sleep in *Per2*^{Luc} mice and the rebound in both variables after SD were similar to those observed in C57Bl/6J mice [control data not shown here but see[3-5]]. See supplementary information for EEG/EMG surgeries and analysis.

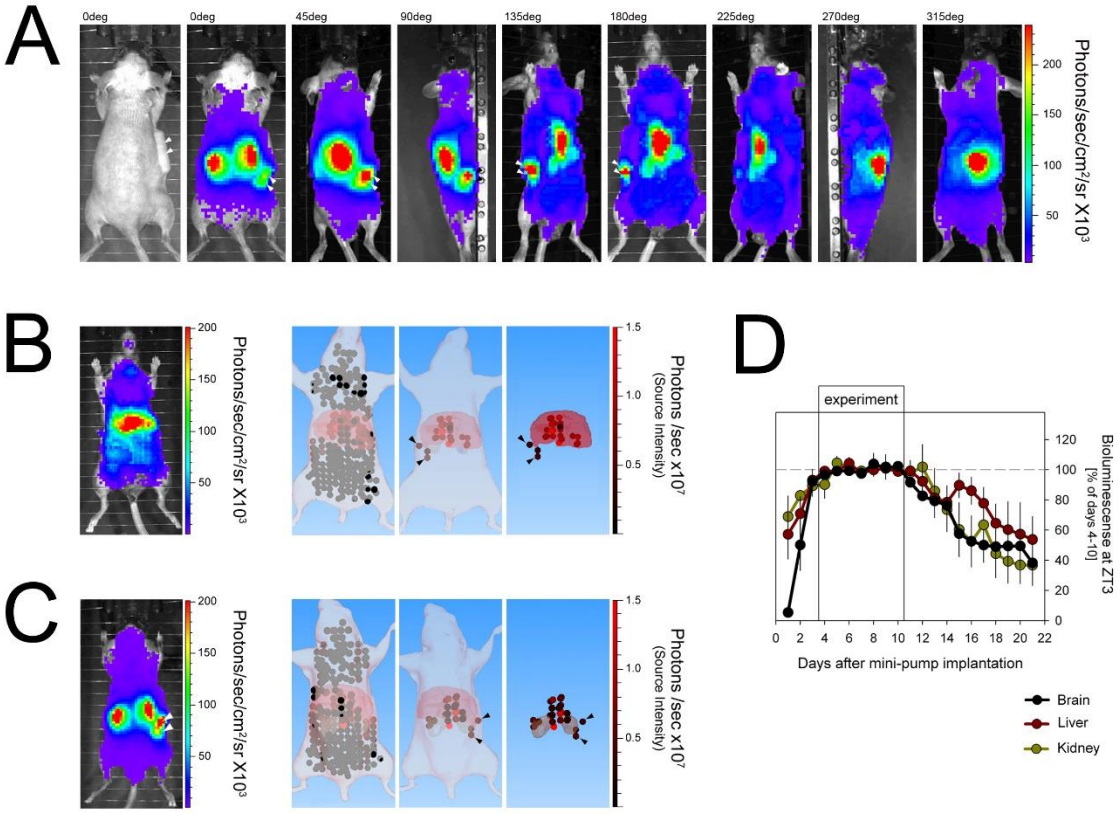

Figure S2: *In vivo* source localization of peripheral PER2 expression in *Per2*^{Luc} mice. **A**: 3D-acquisition of bioluminescent signals was performed at ZT18 with different angular views (0-315° at 45° increments) to localize the bioluminescence source. Mini-pump introduced subcutaneously (white arrowheads in left-hand image) released luciferin in the periphery showing strongest signals in one ventral and two dorsal parts. After 3D-reconstitution (Living Image 3.0; Xenogen), strongest voxels were found to be superposed on the liver (ventral view; **B**) and in the kidneys (dorsal view; **C**). Note that the mini-pump releasing luciferin is also visible (two black arrowheads). **D**: Mean (± 1SEM) bioluminescence levels in brain (black), liver (brown), and kidney (green line) under baseline conditions taken daily at ZT3 for 21 days from the day of mini-pump implantation (i.e., day 0). The "experiment" window indicates the time frame (days 4-10) within which data were collected. Values were expressed as a percentage of the individual average bioluminescence during the days data were collected.

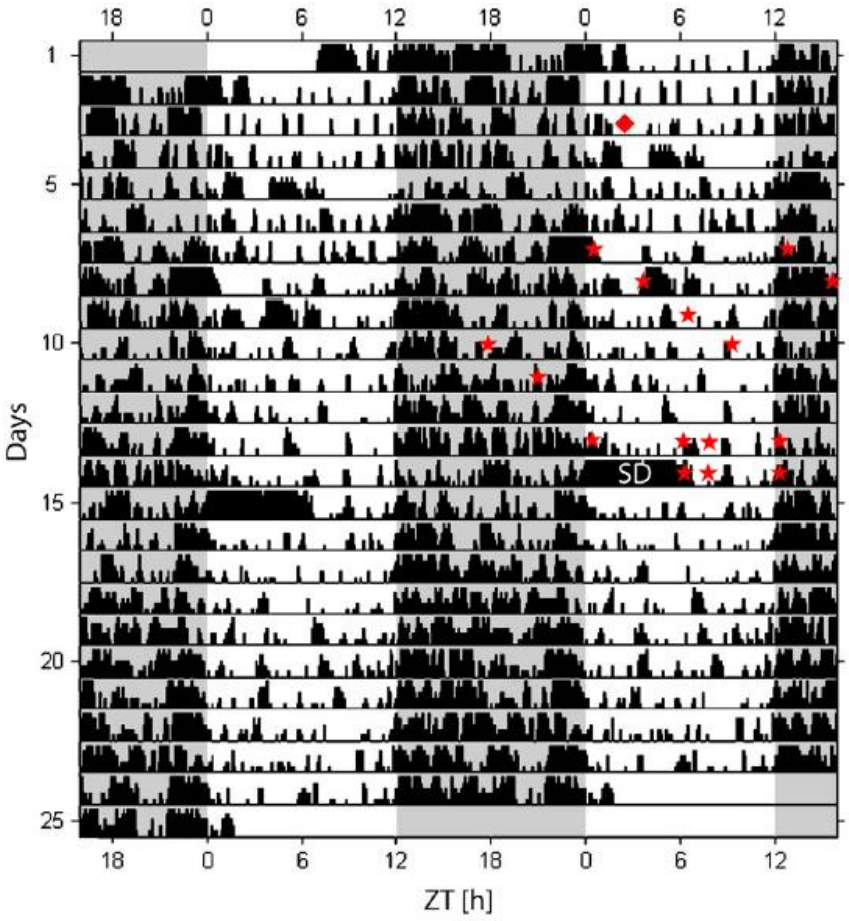

Figure S3: Actogram of double-plotted locomotor activity of one individual *Per2*^{Luc} male under 12:12h light-dark conditions used to sample bioluminescence 15 times (red asterisks) over a 7-day period under baseline conditions (days 1-4: ZT0, -12, -3, -15, -6, -18, -9, -21) and before (day 6: ZT0, -6, -8, -12) and after a 6h sleep deprivation (SD; day 7: ZT6, -8, -12). Red diamond indicates time of mini-pump implantation. Grey areas delineates the dark period. Note that imaging did not importantly alter the nycthemeral organization of activity.

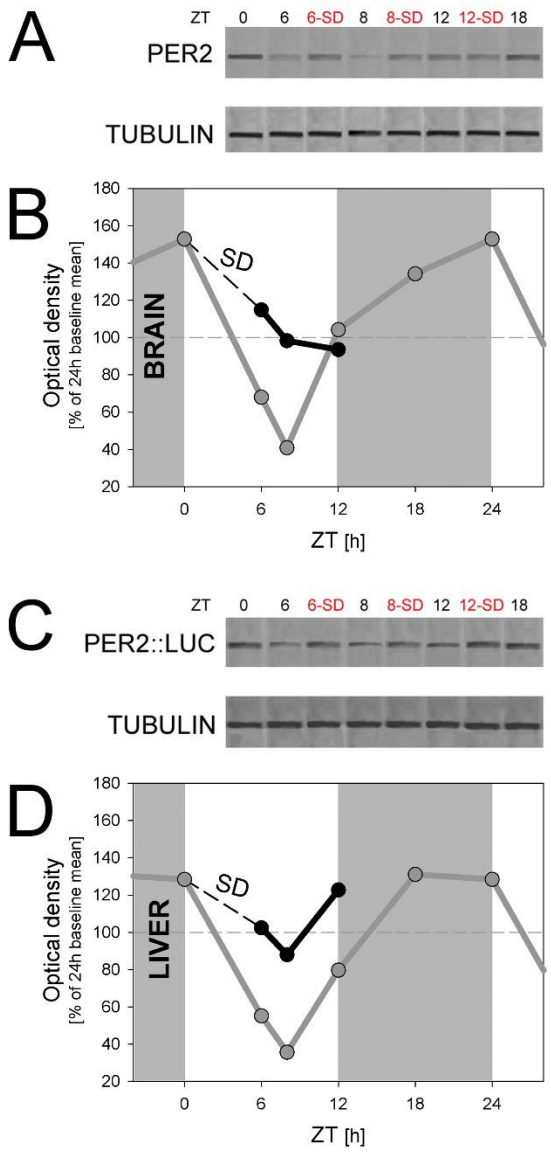

Figure S4: Western-blot analysis of the effects of sleep deprivation and time-of-day on PER2 levels in brain and liver tissues. Whole brain protein extracts in C57BL/6J mice (**A** and **B**) and whole liver protein extracts in *Per2*^{Luc} mice (**C** and **D**) at ZT0 (double plotted at ZT24), -6, -8, -12, and -18 during baseline conditions and 0- , 2- , and 6h after a 6h sleep deprivation (SD; ZT0-6); i.e., at ZT6 (6-SD), -8 (8-SD), and -12 (12-SD) were used. Protein extracts were incubated with antibodies against mPER2 and mTubulin as an internal control (panels A and C). Panels B and D depict densitometric quantification of band intensity expressed as percentage of the 24h-baseline mean. Grey lines connect baseline level, black lines recovery from SD, grey areas delineate the dark periods.

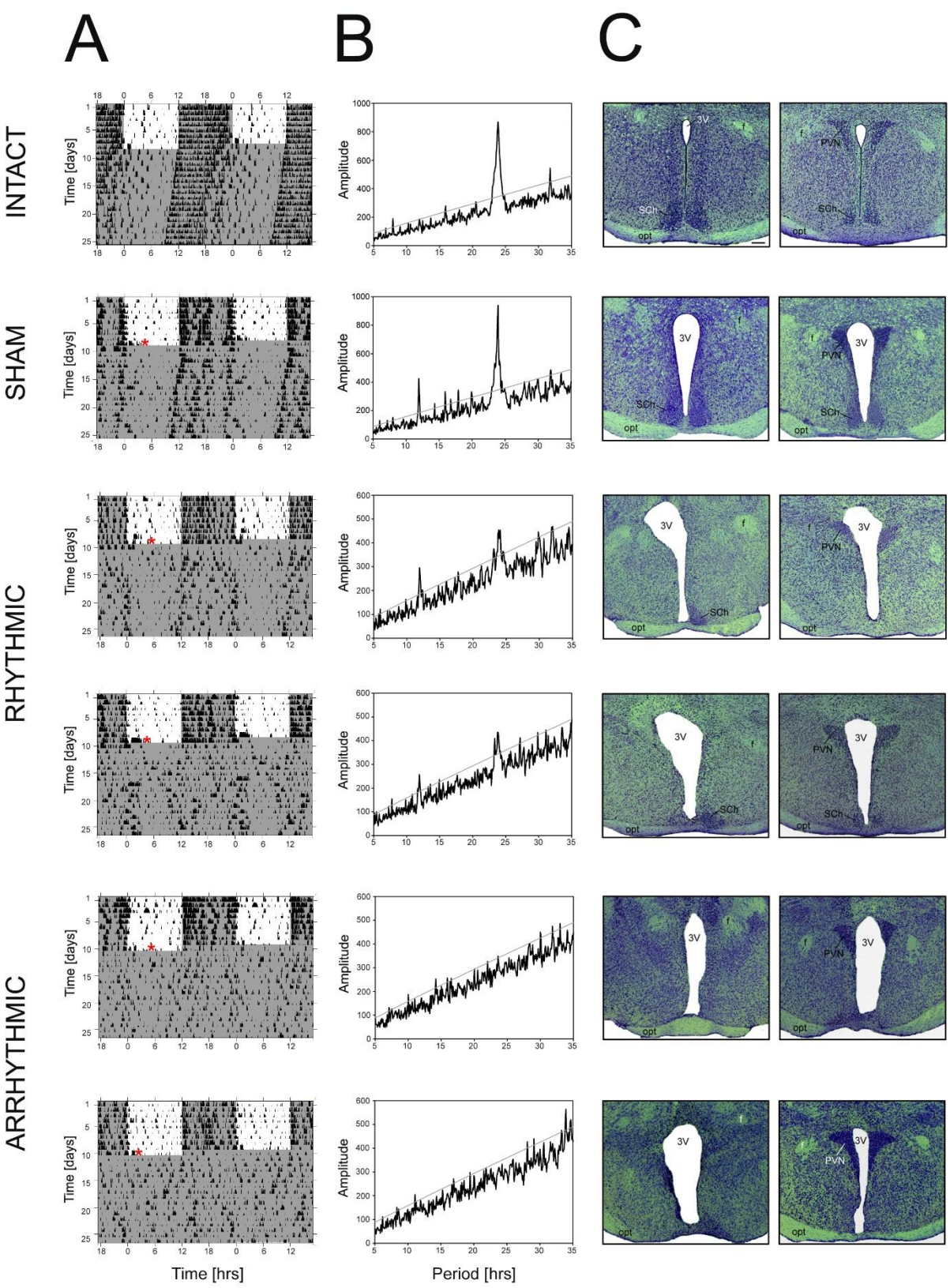
A
B
C
INTACT
SHAM
RHYTHMIC
ARRHYTHMIC
Time [days]
Amplitude
Time [hrs]
Period [hrs]
3V
f
PVN
SCh
opt

Figure S5: Actograms, periodograms, and histology for SCN-lesioned (SCNx) *Per2*^{Luc} mice and their controls. **A**: Double plot of locomotor activity for intact mice, sham-operated mice, and rhythmic and arrhythmic SCNx *Per2*^{Luc} mice. Mice were recorded under 12:12h light-dark conditions for at least 16 days and under constant darkness for at least 17 days in order to verify rhythmicity of each animal. Red stars indicate the time corresponding to the surgery. In sham-operated mice electrodes were inserted but no electrical current was applied. Grey areas delineates the dark period. **B**: Chi-square periodograms (ClockLab analysis software) for the four groups of mice. Grey line marks the Chi-square 5% confidence level. Note that weak but significant circadian rhythmicity was observed in mice with partial SCNx (see C). Also note different scaling of y-axes. **C**: Coronal brain sections performed at two levels of the SCN (-0.46 and -0.82 mm with bregma as a reference according to [6]) in the four groups of mice. Nissl staining in coronal brain section show the absence, partial, and entire presence of the SCN in SCNx-arrhythmic, SCNx-rhythmic, sham, and intact *Per2*^{Luc} mice, respectively. Abbreviations: SCh = SCN; 3V = Third cerebral ventricle; f = fornix; PVN = Paraventricular nucleus; opt = optic chiasm. Scale bar = 200µm.

4. References

1. Franken P, Malafosse A, Tafti M. Genetic variation in EEG activity during sleep in inbred mice. American Journal of Physiology 1998;275(4 Pt 2):R1127-37.
2. Reppert SM, Weaver DR. Coordination of circadian timing in mammals. Nature 2002;418(6901):935-41.
3. Franken P, Malafosse A, Tafti M. Genetic determinants of sleep regulation in inbred mice. Sleep 1999;22(2):155-69.
4. Franken P, Chollet D, Tafti M. The Homeostatic Regulation of Sleep Need Is under Genetic Control. J. Neurosci. 2001;21(8):2610-21.
5. Curie T, Mongrain V, Dorsaz S, Mang GM, Emmenegger Y, Franken P. Homeostatic and circadian contribution to EEG and molecular state variables of sleep regulation. Sleep 2013;36(3):311-23.
6. Paxinos G, Franklin KBJ. The Mouse Brain in Stereotaxic Coordinates. 2nd ed: Academic Press, 2003.